NASA TN D-508

TECHNICAL NOTE
D-508

ANALOG TECHNIQUES FOR MEASURING THE FREQUENCY RESPONSE OF LINEAR PHYSICAL SYSTEMS EXCITED BY FREQUENCY-SWEEP INPUTS

By Wilmer H. Reed III, Albert W. Hall,
and Lawrence E. Barker, Jr.

Langley Research Center
Langley Field, Va.

NATIONAL AERONAUTICS AND SPACE ADMINISTRATION
WASHINGTON
October 1960

1M

TABLE OF CONTENTS

	Page
SUMMARY	1
INTRODUCTION	1
SYMBOLS	2
FREQUENCY-RESPONSE MEASUREMENT TECHNIQUES	6
General	6
Periodic Test Methods	6
Steady-state (constant-frequency) method	6
Quasi-steady (frequency-sweep) method	9
Transient Test Methods	10
Frequency response from transient data	10
Inputs for transient tests	12
SIMULATED FREQUENCY-RESPONSE TESTS	14
Scope	14
Simulated Aeroelastic System	15
Results Obtained With Various Inputs	15
Periodic inputs	15
Quasi-periodic inputs	16
Arbitrary inputs	17
Simulated Flight Flutter Tests	18
Elimination of Errors Due to Sweep	19
FLIGHT VIBRATION TEST RESULTS	19
CONCLUDING REMARKS	21
APPENDIX A - ERRORS DUE TO AVERAGING DEVICE WHEN FREQUENCY-SWEEP INPUTS ARE USED	23
APPENDIX B - FREQUENCY-SWEEP INPUTS DESIGNED TO PRODUCE UNIFORM FREQUENCY SPECTRA	29
APPENDIX C - EQUATIONS OF MOTION FOR THE SIMULATED AEROELASTIC SYSTEM	34
REFERENCES	37
FIGURES	39

NATIONAL AERONAUTICS AND SPACE ADMINISTRATION

TECHNICAL NOTE D-508

ANALOG TECHNIQUES FOR MEASURING THE FREQUENCY RESPONSE OF LINEAR PHYSICAL SYSTEMS EXCITED BY FREQUENCY-SWEEP INPUTS

By Wilmer H. Reed III, Albert W. Hall,
and Lawrence E. Barker, Jr.

SUMMARY

Data-reduction methods using general-purpose analog computer equipment and compatible testing techniques for determining the frequency response of linear physical systems are examined. The techniques considered may be classed as steady state or transient depending on the method of excitation. The relative merits of periodic, slow sweep, and transient (rapid sweep) forcing functions are discussed and applications are given that relate to dynamic-response tests of aeroelastic systems.

Two frequency-sweep-input methods are considered in detail. In one case the sweep rate is sufficiently slow that the response is approximately the same as that for steady-state conditions. With this input the frequency response can be evaluated and displayed in real time while the test is in progress. Errors due to treating sweep data as steady state can be eliminated, when desired, by reanalyzing tape-recorded time histories of the input and output as transient rather than as periodic data. In the second method the frequency-response function is determined from the system's transient response to a very rapid sweep input. The purpose of frequency sweep in this case is to provide sufficient harmonic content in the input to overcome noise while keeping the test time as short as possible. On the basis of simulated forced-response tests and limited flight-test data presented herein, it appears that a transient-type rapid-sweep forcing function offers a considerable saving in test time while preserving the accuracy possible with steady-state sinusoidal inputs.

INTRODUCTION

Frequency-response analysis plays an important role in a variety of problems in dynamics. The literature is replete with applications

of frequency-response methods in such diverse fields as automatic controls, vibration and flutter, chemical processes, heat exchangers, and many others. Excellent surveys of the field are provided in references 1 and 2.

Manual determination of the frequency response of a system from vibration time histories of its input and output is, in general, a tedious time-consuming task which often produces inaccurate results if noise is present in the data. These difficulties have been overcome in recent years by the application of the principle of the wattmeter as a means of harmonic analysis of periodic data. By this method the relative phase angle and amplitude of a data signal with respect to a simple harmonic reference signal can be measured accurately even when the data are contaminated by a high level of noise. The method has been employed successfully in such applications as wind-tunnel testing (refs. 3 and 4), measurement of process dynamics (ref. 5), and structural response measurements (ref. 6).

A requirement which sometimes precludes the use of the wattmeter method is that the measurements be taken during steady-state response of the system to sinusoidal excitation. Often in practice these conditions cannot be satisfied, for example, because of the short duration of a test. If the system is essentially linear and its parameters do not vary with time during a test, it may be more feasible to evaluate the frequency-response functions indirectly from the transient response of the system to known arbitrary inputs. It appears desirable then to consider other techniques applicable to transient as well as to periodic-type frequency-response tests.

Although special-purpose analog equipment has been used for many years for frequency analysis (electrical filters, Fourier analyzers, special slide rules, etc.), general-purpose electronic analog computing equipment has not been widely used. This paper will demonstrate frequency-response data-reduction methods using general-purpose analog computing equipment. The relative merits of sinusoidal, slow sweep, and transient forcing functions are also discussed and application of these techniques are illustrated for aeroelastic systems with particular reference to flight vibration testing.

SYMBOLS

a_j, b_j coefficients in equations of motion

A_n, B_n coefficients in Fourier series

b	semichord of airfoil
C_h	stiffness coefficient of vertical translation spring
C_α	stiffness coefficient of torsional spring
E_o	amplitude of reference signal voltage
$F[\ ]$	Fourier transform of time function in brackets
$F(t)$	normalized forcing function, $\frac{P(t)}{mb\omega_h^2}$
$G(i\omega)$	complex frequency-response function
h	vertical displacement of elastic axis of airfoil
$\bar{h} = h/b$	
I	input to averaging circuit
I_α	moment of inertia of airfoil section about elastic axis
k_h	nondimensional frequency parameter, $\frac{\omega_h b}{U}$
l	aerodynamic lift per unit span
M	Mach number
m	mass
m_a	aerodynamic moment per unit span about elastic axis
n	integral number of sinusoidal oscillations
N_T	normalized input force due to random air turbulence
N_E	pick-up noise added to response
O	output of averaging circuit
P	forcing function
$r_\alpha^2 = \frac{I_\alpha}{mb^2}$	

s	Laplace operator or distance along polar-frequency-response curve
S_α	moment of mass about elastic axis
t	time
$\bar{t} = \omega_h t$	
t_b	time to sweep one bandwidth, $\delta/\dot{\omega}$
t_{in}	duration of arbitrary forcing function
T	fundamental period
U	horizontal velocity of airfoil
w_T	vertical air turbulence velocity
x	periodic function of time
x_o	distance in chord lengths from leading edge to elastic axis
x_α	static unbalance distance in semichords (positive for rearward center of gravity)
y	response of system to an input
z	displacement of airfoil leading edge, in semichords
α	angular rotation of airfoil about elastic axis
δ	bandwidth of second-order system, $2\zeta\omega_n$
Δ	increment
ζ	damping ratio in percent of critical damping
θ	arbitrary initial phase angle of reference signals
μ	density ratio of airfoil section, $\frac{m}{\pi\rho b^2}$
ρ	air density
τ	time constant of averaging device

φ	phase lag of response relative to input
ψ	phase shift of averaging device
ω	frequency, radians/sec
ω_h	frequency, uncoupled vertical translation
ω_α	uncoupled torsional frequency
ω_n	undamped natural frequency of second-order system
$\bar{\omega} = \frac{\omega}{\omega_h}$	
ω_1	average frequency (eq. (B2))
$\lvert\ \rvert$	amplitude of complex quantity

Subscripts:

f	final value
i	initial value
I	imaginary part of complex quantity
o	amplitude of oscillation
R	real part of complex quantity
s	frequency sweep
st	static deflection
τ	time constant
av	average
max	maximum

An arrow over a symbol denotes a time vector. Dots over symbols indicate derivatives with respect to t. Primed symbols denote derivatives with respect to $\bar{t}$.

FREQUENCY-RESPONSE MEASUREMENT TECHNIQUES

General

Techniques for measuring the frequency response of physical systems may be grouped into three categories according to the type of forcing function used. These forcing functions are defined as (a) steady-state periodic, (b) arbitrary transient, and (c) continuous random. If the system is linear and its parameters do not vary with time, the measured frequency response is, in the absence of noise, independent of the testing technique used. In this paper the steady-state periodic and transient test methods are considered and the system is always assumed to be linear.

Periodic Test Methods

Steady-state (constant-frequency) method.- When the application of the wattmeter principle as a method of measuring frequency response with periodic excitation is considered, it is helpful to look at the Fourier series expression for a periodic function. If $x(t)$ is periodic in the interval T, it may be defined over the interval by a Fourier series expansion as follows:

$$x(t) = \frac{A_o}{2} + \sum_{n=1}^{\infty} (A_n \cos n\omega t + B_n \sin n\omega t) \tag{1}$$

where

$$A_n = \frac{2}{T} \int_0^T x(t) \cos n\omega t \, dt$$

$$B_n = \frac{2}{T} \int_0^T x(t) \sin n\omega t \, dt$$

and

$$T = \frac{2\pi}{\omega}$$

Each harmonic component of $x(t)$ can be looked upon as a vector in a complex plane. The real component is represented by A_n and the imaginary component by B_n (see sketch)

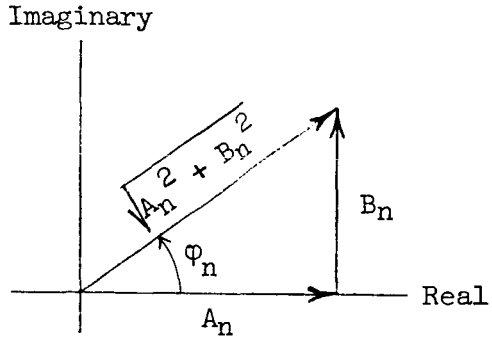

The vector may be expressed in rectangular coordinates as

$$\vec{x}(in\omega) = A_n + iB_n \tag{2a}$$

or in polar form

$$\vec{x}(in\omega) = \sqrt{A_n^2 + B_n^2}\, e^{i\varphi_n} \tag{2b}$$

where

$$\varphi_n = \tan^{-1} \frac{B_n}{A_n}$$

A wattmeter is a device that responds to the average of the product of two applied signals. Thus, if one of these signals is $x(t)$ and the other is $E_o \cos \omega t$, then the quantity indicated by the wattmeter will be proportional to the Fourier coefficient A_1

$$\left[x(t)E_o \cos \omega t\right]_{av} = \frac{E_o}{2} A_1 \tag{3a}$$

and similarly for the coefficient B_1

$$\left[x(t)E_o \sin \omega t\right]_{av} = \frac{E_o}{2} B_1 \tag{3b}$$

Actually, a wattmeter indicates a product averaged over some effective averaging time which is dependent upon the time constant of the averaging device. If the time constant is too small, the output fluctuates and makes it difficult to read a mean value. On the other hand, if the time constant is too large, the time required to establish steady-state conditions may be prohibitive. A suitable compromise generally

results if the time constant is from 3 to 6 times greater than the period of the signal being analyzed.

If $y(t)$ is the steady-state response of a system due to a sinusoidal input $P(t)$, the frequency-response function is determined by the vector ratio

$$\left.\begin{aligned} G(i\omega) &= \frac{\vec{y}(i\omega)}{\vec{P}(i\omega)} \\ G(i\omega) &= \frac{y_R + iy_I}{P_I + iP_I} \end{aligned}\right\} \qquad (4a)$$

or in polar form

$$G(i\omega) = \frac{\sqrt{y_R^2 + y_I^2}}{\sqrt{P_R^2 + P_I^2}}\, e^{-i\varphi} \qquad (4b)$$

where φ is the angle by which the response lags the input.

Figure 1 illustrates the application of the wattmeter principle in the determination of the vector components of frequency response for a system. For the case shown it is assumed that the input is a pure sine wave of amplitude P_o. In the more general case, where the forcing function may be contaminated by harmonics, it would be necessary to analyze the input as well as the output by using sinusoidal reference signals the frequency of which is the fundamental of the input.

In practical applications, the operations indicated in the figure have been mechanized in a variety of ways. Some examples are thermocouple wattmeters, vacuum tube wattmeters (ref. 3), resolvers and averaging circuits (ref. 4), and electronic analog computer components (ref. 5).

Resolvers provide a particularly simple means of multiplying the response signal by a sine and cosine reference signal in cases where the resolver can be mechanically connected to a rotating shaft having the same angular frequency as the excitation frequency. In other methods (ref. 6), strain-gage transducers serve as the multiplying device when the bridge-circuit is powered by a sinusoidal reference signal. Averaging of the product may be accomplished by low pass

electrical filters, or by measuring the output on a long-time-constant D'Arsonval meter.

It should be pointed out that the accuracy of the wattmeter technique is governed by the quality of the simple harmonic reference signals. If these signals contain harmonic distortion or oscillate about a mean value other than zero, the indicated vector components will be in error. The magnitude of the error is shown in reference 4 to be equal to one-half the sum of the products of harmonics (including the zero-frequency component) common to both signals.

Quasi-steady (frequency-sweep) method.- The frequency-sweep technique provides a convenient means of measuring the frequency response of a system when a broad band of frequencies is to be surveyed. With this technique, instead of measuring the steady-state response at various discrete frequencies, the excitation frequency is varied slowly (quasi-steady state) with time. Frequency sweep, used in conjunction with the wattmeter method of harmonic analysis, makes it possible to display a continuous plot of the frequency-response vectors while the test is in progress. This not only affords a saving in test time but also serves to point up areas of particular interest that may otherwise have been overlooked in surveying the frequency range in discrete steps.

Because of the time-varying nature of the input frequency, the observed response of the system at any instantaneous frequency will differ somewhat from the corresponding steady-state response. The effects of frequency sweep on the response for the case of a single-degree-of-freedom system has been investigated by Hok (ref. 7) and by Barber and Ursell of the British Admiralty Research Laboratory (not generally available) where it is shown that in the vicinity of resonance the major effect of sweep is to make the measured maximum response less than the corresponding steady-state maximum and to shift the frequency of maximum response in the direction in which the frequency is changing. These errors, Δy_s and $\Delta\omega_s$, are indicated in figure 2 and some results of Barber and Ursell are plotted in figure 3(a) to show the variation of these errors with a nondimensional sweep parameter $\dot{\omega}/2\zeta^2\omega_n^2$.

When the wattmeter method is used as a means of analyzing frequency-sweep data, additional errors are incurred because of the lag characteristics of the averaging device. (See fig. 2.) An approximate analysis of these errors, denoted as Δy_τ and $\Delta\omega_\tau$ is given in appendix A for a single-degree-of-freedom system. In figure 3(b) the magnitude of such errors is shown plotted against τ/t_b where τ is the time constant of the averaging device and t_b is the time required to sweep

through one bandwidth $(2\zeta\omega_n)$ of the system. The data points on the figure were determined from analog-computer results to be described later in the paper and serve to confirm the predictions of the approximate analysis in appendix A.

Transient Test Methods

Frequency response from transient data.- As mentioned before, it is not always feasible to use steady-state sinusoidal inputs in frequency-response tests. Such a procedure would obviously be impractical in such cases as flight tests of a missile system. Here not only is the time available for testing short but also the dynamic characteristics and environment of the system may be varying with time so that a steady-state response could never be obtained. Under these circumstances it is necessary to abandon test methods based on steady-state concepts and consider instead methods of determining frequency response from transient data. (It must still be assumed that the system is time-invariant. This assumption implies that, although the system's parameters may vary with time, the variations occurring during the transient response to an input are insignificant.)

Just as the Fourier series provides the mathematical basis for analyzing steady-state response measurements, the Fourier transform provides the basis for analyzing transient phenomena. The frequency-response function for the transient-type test is determined by dividing the Fourier transform of an arbitrary input into the Fourier transform of the response caused by this input. If the input is applied at time equal zero and the system is assumed to be at rest before this time, the frequency response of the system is defined by the equation:

$$G(i\omega) = \frac{\int_0^\infty y(t)e^{-i\omega t}dt}{\int_0^\infty P(t)e^{-i\omega t}dt} = \frac{F[y(t)]}{F[P(t)]} \qquad (5)$$

In order to evaluate the integrals (Fourier transforms) in equation (5), it is necessary that the response and the input approach some final state for which the integral can be evaluated as time approaches infinity.

A variety of numerical methods for evaluating the Fourier transform of arbitrary time functions have been developed. (See, for example, refs. 8 to 10.) The approach taken in this paper will be to consider analog methods for evaluating these integrals. Specifically, it is desired to modify the techniques discussed previously for the analysis

of periodic data so that, insofar as possible, the same equipment could be employed for the analysis of transient time histories.

Consider first the case where the system after being disturbed returns to its original state of static equilibrium. Let $y(t)$ and $P(t)$ in equation (5) represent perturbations from static equilibrium and t_f be the time required for the transient oscillations to subside. The upper limits of integration in equation (5) can then be replaced by t_f without affecting the results. Therefore, with the relation

$$e^{-i\omega t} = \cos \omega t - i \sin \omega t$$

equation (5) becomes

$$\left.\begin{aligned} G(i\omega) &= \frac{\int_0^{t_f} y(t)\cos \omega t \, dt - i \int_0^{t_f} y(t)\sin \omega t \, dt}{\int_0^{t_f} P(t)\cos \omega t \, dt - i \int_0^{t_f} P(t)\sin \omega t \, dt} \\ G(i\omega) &= \frac{F\left[y(t)\right]_R - iF\left[y(t)\right]_I}{F\left[P(t)\right]_R - iF\left[P(t)\right]_I} \end{aligned}\right\} \qquad (6)$$

The mathematical operations for evaluating the Fourier transforms in equations (6) are illustrated by the block diagram in figure 4. Note the similarities between these operations and those indicated in figure 1 for the case of sinusoidal forcing functions. In each case a data signal is multiplied by a pair of sinusoidal reference signals phased 90° apart. Whereas with sinusoidal excitation the frequency of the reference signal is the same as the driving frequency, with transient excitation it may be any value in the frequency range of interest. A second difference in the two methods is that the averaging circuit used in the periodic case is replaced by an integrating device.

From equations (6) it is seen that the frequency-response function is determined from the complex ratio of the values of the integrated products at the time t_f. Also, it should be pointed out that the initial phasing between the sine-cosine reference signal and the data signals (indicated by θ in fig. 4) is unimportant so long as the same pair of reference signals is used to analyze both the input and the output time histories. Since phase is relative, the choice of a time base is unimportant.

Equations (6) were derived on the assumption that, after some finite time interval t_f, the system returns to the same static equilibrium state that existed before the disturbance was applied. In event the initial and final static equilibrium are different, such as with step-function inputs, it is necessary to account for this difference in a manner indicated in reference 8. The modified form of equations (6), which is applicable when the final values of $y(t)$ and $P(t)$ are constants other than zero, is:

$$G(i\omega) = \frac{\left\{F\left[y(t)\right]_R - \frac{y(t_f)\sin \omega t_f}{\omega}\right\} - i\left\{F\left[y(t)\right]_I + \frac{y(t_f)\cos \omega t_f}{\omega}\right\}}{\left\{F\left[P(t)\right]_R - \frac{P(t_f)\sin \omega t_f}{\omega}\right\} - i\left\{F\left[P(t)\right]_I + \frac{P(t_f)\cos \omega t_f}{\omega}\right\}} \qquad (7)$$

With the transient testing method it is desirable, although not essential, to record the time-history data on magnetic tape. Then, a short burst of data from a single test is sufficient to determine the frequency response over the range of frequencies present in the input. The frequency response would be obtained by playing the data repeatedly into the transient analyzer, while changing the frequency of the reference signals before each pass. Without the benefits of magnetic tape, the test must be repeated with each change of the reference signal frequency, a situation analogous to the test procedure normally used with sinusoidal inputs.

Inputs for transient tests.- In the determination of frequency response from transient tests, the range of frequencies that can be analyzed with accuracy depends on the harmonic content of the input.

The frequency spectra of a half-sine-wave pulse and a step function are plotted in figure 5 and are representative of inputs often used in practice. (See ref. 2.) Note that the frequency content of these functions falls off with increasing frequency. For the half-sine pulse, and also other symmetrical pulse shapes, the frequency content even goes to zero (bottoms) periodically. Thus, with noise present in the data the accuracy of frequency-response measurements is likely to deteriorate at frequencies where the harmonic content of the input is low.

In order to extend the frequency range beyond that provided by pulse inputs, a manual frequency-sweep technique for determining airplane frequency response is investigated in reference 11. In these tests the pilot oscillated the airplane longitudinal control system at a continuously increasing rate so that in only 5 or 10 cycles the period of the input control motion varied from 3 to 0.3 seconds. The harmonic content of the input in the frequency range covered by the sweep was found to be appreciably higher than that of a triangle input used for

comparison everywhere except at the natural frequency of the airplane pitching mode. At this resonant frequency the pilot apparently reduced the input to avoid excessive airplane pitching oscillations.

The harmonic content of a frequency-sweep input is dependent not only on the amplitude of the input and the frequency range swept but also on the manner in which the frequency varies with time through this range. It should be possible, therefore, to program the variation of frequency with time in such a way that the harmonic content of the signal is approximately uniform over frequencies covered by the sweep. This procedure is somewhat analogous to the use of "white noise" excitation (uniform power spectral density) in tests involving random inputs. In the present case, however, the aim is not only to achieve a uniform spectrum but also to economize on testing time by building up the necessary frequency content of the input as rapidly as possible.

The problem of designing frequency-sweep inputs which have uniform frequency spectra is treated in appendix B. Three variable-frequency constant-amplitude functions are considered: a sine wave, a sawtooth function, and a rectangular pulse train (see sketch (b) of appendix B). It is shown that for such functions a linear variation of frequency with time produces a uniform spectrum. For a given frequency-sweep range the level of the spectrum is proportional to the square root of the sweep time. Thus if t_{in} is the time required to increase the frequency of the input from an initial value ω_i to a final value ω_f the effective level of the spectrum over these frequencies is, from appendix B,

$$\left|F\left[P_o(t)\right]\right| = KP_o\sqrt{\frac{t_{in}}{\omega_f - \omega_i}} = \frac{KP_o}{\sqrt{\dot{\omega}}} \tag{8}$$

where for the sine function $K = \sqrt{\frac{\pi}{2}}$, for the sawtooth function $K = \sqrt{\frac{\pi}{3}}$, and for the rectangular-pulse function $K = \sqrt{\pi}$.

The spectrum of a frequency-modulated sine function is shown in figure 5. The circle data points represent the true spectrum as determined by an analog computer and shown for comparison is the effective spectrum level predicted by equation (8) with $K = \sqrt{\frac{\pi}{2}}$. Good agreement between the true and the effective levels is indicated everywhere over the sweep-frequency band except near the end frequencies ω_i and ω_f where the actual spectrum is about one-half the effective value. This difference might be expected when one considers that the end frequencies have adjacent frequencies only on one side.

Since the use of frequency sweep has been discussed both from the standpoint of periodic and transient type testing, it is of interest to compare the criteria for selecting a sweep rate for the two cases. For the periodic case the object is to sweep at a rate sufficiently slow that the system behaves essentially as it would if conditions were steady. If the system is lightly damped or if its natural frequencies are closely spaced, this criterion may require that extremely slow sweep rates be used.

With the transient testing technique, the major concern is simply that there be sufficient harmonic content in the input to excite the system above whatever noise may be present. Beating between frequencies of closely spaced natural modes presents no difficulty so long as the system is disturbed from and returns to steady-state conditions and the entire transient time history is included in evaluating the Fourier transforms. Since in the transient case it is unnecessary to establish, or even approach, steady-state conditions during the sweep, the time required to accomplish the sweep can be less by an order of magnitude or so than the sweep time normally used for the quasi-periodic case.

L 9 8 5

SIMULATED FREQUENCY-RESPONSE TESTS

Scope

In previous sections of the paper various techniques were discussed for automatically determining the frequency response of physical systems. The aim of the present section is to demonstrate the application of these techniques with a specific example, the example chosen being the forced response of a simple aeroelastic system in supersonic flow. For this purpose both the aeroelastic system and the harmonic analyzer used to evaluate its frequency response were simulated on an analog computer as illustrated in figure 6. By using the data-reduction techniques discussed earlier, the frequency response of the system was evaluated for three methods of excitation: periodic, slow sweep, and transient rapid sweep.

In order to gain some insight into the noise-rejection capabilities of these data-reduction techniques, simulated atmospheric turbulence and instrumentation pick-up noise were introduced in some cases. As indicated in figure 6, the noise could be switched on or off at will so that the effects of noise on the final result could be easily observed.

Also, since in practical applications of the sinusoidal excitation method pure sine-wave forcing functions are often not realized because of, say, nonlinear elements in the force-generating mechanism, provisions were made for introducing harmonic distortion into the input.

Simulated Aeroelastic System

The aeroelastic system simulated on the computer was a two-degree-of-freedom flat-plate airfoil which is shown schematically in figure 7. The equations of motion, developed in appendix C, utilize piston theory (ref. 12) at a Mach number of 2.0 for defining the aerodynamic forces. In all cases the forcing function was assumed to act at the leading edge of the airfoil and the response was taken to be the vertical displacement at this point. The frequency response of the system and the test conditions are given in figure 8. In this figure the amplitude ratio is the leading-edge displacement normalized with respect to the static deflection of the elastic axis and the phase angle is the angle by which the displacement lags the force. The solid curves in the figure represent the theoretical frequency response determined from the equations of motion and the points are typical results obtained with transient and periodic inputs. These results indicate the overall accuracy and the repeatability of the simulation in the absence of noise.

In order to simulate atmospheric turbulence the output of a Gaussian "white noise" generator was passed through a low-pass filter. By adjusting the filter time constant the frequency content of the filter output was matched to that measured for atmospheric turbulence in reference 13. Similarly, instrumentation pick-up noise was simulated with another filter which passed considerably higher frequencies than the filter for air turbulence. Plots of the power spectral density of the simulated turbulence and pick-up noise used throughout the paper are given in figure 9.

Results Obtained With Various Inputs

Periodic inputs.- Consider first the case in which the system is driven by a periodic forcing function. Typical analog time histories showing the input, the response, and the corresponding vector components are given in figure 10. The forcing function for this case had a fundamental frequency of 1.9 radians per second plus appreciable harmonic distortion representing nonlineariaties in the force-generating device.

For discussion purposes the figure is divided into three time intervals. The first interval shows the behavior of the system with no random noise present. In the second time interval atmospheric turbulence was added and also the recorder speed was increased. The magnitude of the aerodynamic force due to turbulence, shown by the bottom trace N_T in figure 10, has a root-mean-square value some 3 times that of the periodic forcing function. (The force scales for $F(t)$ and N_T are the same in the figure.) Its effect on the vector components of

response, however, is practically negligible because of the low frequency content of turbulence at the frequency being analyzed $\left(\omega/\omega_n = 1.9\right)$. (See fig. 9.) In the third interval simulated pick-up noise N_E was added to the output. The frequency content (fig. 9) and intensity of the pick-up noise were adjusted by trial and error to make $z(t)$ appear representative of "noisy" experimental data. For the case shown, the maximum excursion of the $z(i\omega)$ vector due to noise is in the imaginary component and is approximately 15 percent of the vector length.

Quasi-periodic inputs.- Consider next a sinusoidal forcing function of slowly varying frequency. Figure 11(a) shows the time-history response and the vector components of the simulated system excited by an input of linearly increasing frequency. In order to emphasize the effects of sweep alone, random noise and harmonic distortion in the input were not included here.

It is of interest to compare the vector components indicated by the analyzer with the theoretical steady-state components which are shown by the dashed curves. Note that the effects of sweep, previously illustrated in figure 2 and appendix A, are clearly evident. Subsequently, it is shown how such errors can be eliminated by analyzing slow sweep time histories as transient rather than as quasi-steady-state data.

Figure 11(b) shows a polar plot of the same vector components given in figure 11(a). This curve was obtained by feeding the real and imaginary vector components to an X,Y plotter. The plot represents the locus of the tip of the frequency-response vector as the input frequency varies. The amplitude ratio is given by the vector length and the phase angle, by the angle between the vector and the positive real axis. Again, the theoretical steady-state values are shown for comparison.

The two natural modes of the system may be identified in figure 11(b) by the two circular-shaped loops. The inner loop is associated with the vertical translation mode while the outer loop is associated with the torsion mode. In considering ground vibration tests of airplanes, Kennedy and Pancu (ref. 14) developed methods for evaluating damping and natural frequencies from the near-circular shapes exhibited by the vector polar plot of frequency response. Broadbent (ref. 15) also applies the method to flight flutter testing as a means of determining the damping from flight-forced-response tests.

In order to identify natural frequencies by the polar-plot method, Kennedy and Pancu suggest use of the variation of distance along the polar curve for equal frequency increments. Natural frequencies occur where $ds/d\omega$ is a maximum, s being the distance along the polar curve. For complex systems this method is found to give a better indication of natural frequencies than do the frequencies of maximum response. Note

in figure 11(b) that, with frequency sweep, the polar plot is generated by many small coil-like loops. These loops arise from a ripple passed by the averaging filter and can serve to provide a convenient measure of $ds/d\omega$. In order to illustrate, let Δs be the distance between adjacent loops. The time Δt required for the vector to describe one loop is one-half the period of the forcing frequency (there are two ripple cycles for each input cycle); therefore,

$$\Delta t = \frac{\pi}{\omega}$$

and

$$\Delta\omega = \dot{\omega}\Delta t$$

These relations combine to give

$$\frac{ds}{d\omega} \approx \frac{\omega\Delta s}{\pi\dot{\omega}} \tag{9}$$

Figure 11(c) is a duplicate of figure 11(b) except for the addition of turbulence and electrical pick-up noise. For the noise levels used, the two cases are in good agreement at all frequencies.

Arbitrary inputs.- For the case of arbitrary forcing functions, the input and transient response of the system were analyzed by the procedure shown in figure 4. In this simulated study the input was repeated each time the reference frequency was changed. In testing an actual physical system, however, it would be more feasible to perform only one test and record the data on magnetic tape which would then be played repeatedly into the transient analyzer (fig. 4) for evaluation of the frequency response.

The transient response of the system to a half-sine-wave pulse and a rapid-sweep input are illustrated in figure 12. Time histories such as these were used to determine the amplitude and phase angle of frequency response indicated by the circular data points in figure 8. Since no noise was present, the pulse and the sweep data gave identical results. With the addition of random noise, however, the accuracy of the results depends on the ratio of the harmonic content of the signal to that of the noise at the frequency being analyzed. Thus, as discussed previously (see fig. 5), for a given noise level the rapid sweep input would produce more accurate results than the pulse input.

Results of the analysis of a typical transient response with noise added is given in figure 13. In order to obtain the frequency response (the case shown is for $\omega/\omega_h = 2.0$ radians/sec), a complex ratio is taken between $F\left[z(t_f)\right]$ and $F\left[F(t_f)\right]$ where the subscript f denotes

the final value after the transient motion has damped out. Note that, because of the effects of simulated turbulence and pick-up noise, there are small random fluctuations in the final values of the Fourier transform of response. These errors have maximum value of about 4 percent for the case shown. With a slower sweep rate, such as shown in figure 5, the frequency content of the input would be greater and therefore the percentage error would be reduced. If the half-sine pulse had been the input, the same noise intensity would give rise to errors of the order of 20 percent.

Simulated Flight Flutter Tests

Up to this point all the results presented have been for a single set of parameters. (See key in fig. 8.) Generally, one purpose of any dynamic-response test is to examine how changing various parameters affects the performance or stability of the system being tested. In the case of flutter testing, for example, it is of interest to determine not only whether the system is free from flutter for a given test condition, but also to have some indication of the degree of stability. Since flutter is often explosive in nature and generally leads to catastrophic structural failures, it is highly desirable to have a means of assessing response of the test vehicle while the test is in progress so that tendencies toward instability can be readily observed.

It is of interest to illustrate how some of the frequency-response testing and automatic data-reduction techniques described in this paper might be applied to flight flutter tests. For this purpose, the density ratio μ in the equations of motion for the aeroelastic system (see appendix C) was varied to represent flights at various altitudes. A slow sweep run was made at each altitude and the frequency-response vector components were automatically plotted on an X,Y plotter while the test was in progress. The results are shown in figure 14. The plot in the upper left of the figure is the basic configuration ($\mu = 20$) shown in figure 11(b). Note that, as μ approaches the critical flutter value, which is 8.3, the circular shapes associated with the two natural modes of the system tend to lose their individual identity and the response takes on the appearance of that of a single-degree-of-freedom system.

This apparent merging of two natural modes as a flutter condition is approached is characteristic of a large class of flutter phenomena. In reference 16, the concept of frequency coalescence of natural modes is used to provide a simple explanation of the mechanism of flutter.

Elimination of Errors Due to Sweep

As discussed previously, the vector plots in figure 14 are in error due to the effects of frequency sweep. Even though such errors exist, plots of this type are of considerable value in that they make possible a qualitative assessment of the data while the tests are in progress. Often, when systematic variations of parameters are made, it will be found that many of the runs turn out to be of little interest and do not warrant further consideration. However, for the most significant cases it would be desirable to have a means of eliminating the errors due to sweep. This can be done by performing a transient analysis after the test if the sweep time histories, including transients at the beginning and end of the sweep, are recorded on magnetic tape.

Thus, a proposed testing technique using slow-sweep excitation would be to obtain first a qualitative "quick-look" at the frequency response during the test by the periodic method of analysis. Then, after completion of a series of runs, those that appear to be the most significant would be reanalyzed at discrete frequencies by the transient method to correct for the errors caused by analyzing sweep data as though it were steady-state data.

FLIGHT VIBRATION TEST RESULTS

In this section of the paper the frequency-response measurement techniques discussed earlier are applied in flight tests involving aeroelastic response measurements of a jet airplane. The predominant symmetrical vibration modes of the airplane were excited by servo-controlled inertia shakers installed in each wing tip and the resulting wing-tip acceleration measured. A further description of the test equipment may be found in reference 17.

As in the simulated forced-response tests, three types of forcing functions were used - steady-state sinusoidal, slow sweep with frequency increasing from 4.5 to 40 cycles per second in 30 seconds, and a rapid sweep in which the same frequency range is swept in only 6 seconds. (For reasons not pertinent to this discussion, the sweep rate was programed to increase as the square of the frequency for both the slow- and the rapid-sweep cases.) The frequency-response function was evaluated in each case by playing tape-recorded time histories of the shaker force and wing-tip acceleration response into an analog computer. Typical frequency-response plots for the three methods of excitation are shown in figure 15.

The sinusoidal and slow-sweep data were analyzed by the periodic method (fig. 1) and rapid-sweep data were analyzed as transients (fig. 4).

For the periodic case the reference signals were obtained from the signal generator used to drive the shaker servo system. High-speed electronic multipliers were used to multiply the reference signals by the data signals; thus, the data could be reduced in real time.

For the transient case the electronic multipliers were replaced by an electro-mechanical device which, in addition to performing the multiplication operation, also generated the reference signals. This was accomplished by driving a pair of d-c sine-cosine potentiometers (see ref. 18) with a constant-speed electric motor as illustrated in figure 16(a). A sine-cosine potentiometer is a device which, when rotated at a speed ω, generates the products $\pm A \cos \omega t$ and $\pm A \sin \omega t$, where $+A$ and $-A$ are analog voltage signals applied across windings of the potentiometer. In the present case these applied voltages are proportional to the shaker force $P(t)$ and the acceleration response $\ddot{y}(t)$. As shown in the figure the two potentiometers are geared together and driven by a common shaft whose rotational speed could be set at any desired value of ω from 0 to 40 cycles per second. A photograph of the actual device used is shown in figure 16(b). L 9 8 5

A typical record showing the rapid-sweep time-history data and the corresponding Fourier transforms for a reference signal frequency of 31.2 cycles per second is presented in figure 17. (Note similarity to simulated transient tests shown in fig. 13.) The wing was disturbed from static equilibrium by a sudden application of shaker force which increased in frequency from 4.5 to 40 cycles per second in about 6 seconds. At the end of this time, the shaker was stopped and the response was allowed to dampen out. Actually, the time required to perform the test was governed by the maximum sweep rate of the shaker input signal generator. With the noise level present in these tests, it is felt that a sweep rate several times faster than the one shown could have been used without adversely affecting the accuracy of the results. The four upper traces in the figure are the real and imaginary components of the Fourier transforms of the time histories $P(t)$ and $\ddot{y}(t)$. Although the final values of the Fourier transforms are needed for evaluating frequency response, it is of interest to note that the only time these quantities show appreciable variation is when the frequencies of the shaker and reference signals are close together.

When the frequency-response data in figure 15 are compared, it is seen that the results from each of the three methods of excitation are in reasonably good agreement. The first symmetric wing bending mode of the airplane occurs at 6.8 cycles per second. Also a torsion mode exists at 33 cycles per second but unfortunately the pick-up location was near the node line so that the response of this mode is not readily apparent in the figure.

On the basis of these results it appears that, in aeroelastic dynamic response investigations of aircraft and missiles, a programed transient-type rapid-sweep excitation makes possible a considerable saving in test time while preserving the accuracy of steady-state sinusoidal methods.

CONCLUDING REMARKS

Data-reduction methods using general-purpose analog computing equipment and compatible testing techniques for determining the frequency response of linear physical systems were discussed. The techniques considered were classified as steady state or transient depending on the method of excitation.

When the excitation frequency is varied slowly with time, both techniques of data reduction can be used to advantage. The data are first analyzed by the quasi-steady-state method to permit a cursory examination of the frequency response while the test is in progress. Because true steady-state conditions are not realized, because of the time-varying nature of the input frequency, these results are in error. In order to eliminate such errors from those cases of particular interest, the input-output time histories, having been recorded on magnetic tape, are reanalyzed at discrete frequencies by the transient analysis technique.

A frequency-sweep input is also considered as a forcing function for the transient-type tests. However, in this case the object is not to approach steady-state sinusoidal conditions but rather to build up high concentrations of frequency content over the frequency range of interest while keeping the test time as short as possible. The frequency-response function is then determined after the test by taking the Fourier transform of the input and output time histories. It is shown that linear variations of frequency with time produce uniform frequency spectra the magnitude of which is inversely proportional to the square root of the sweep rate.

As a means of illustrating the techniques considered in the paper, examples are given that relate to the dynamic forced response of aeroelastic systems. In one case the methods are demonstrated for a simple two-degree-of-freedom system that was simulated on an analog computer. In another case flight-test-forced dynamic-response measurements on a jet airplane are analyzed. These examples also serve to indicate the

suitability of using conventional electronic analog computer components in the analysis of experimental dynamic data.

Langley Research Center,
National Aeronautics and Space Administration,
Langley Field, Va., June 15, 1960.

APPENDIX A

ERRORS DUE TO AVERAGING DEVICE WHEN FREQUENCY-SWEEP INPUTS ARE USED

In the wattmeter principle of harmonic analysis, the power or product read by a wattmeter varies over any cycle; thus, an averaging device is needed to secure the average or mean power over a number of cycles. In the case of frequency sweep the mean value varies with time and the output of the averaging device tends to lag the true mean value. This lag, together with the frequency-sweep effects analyzed by Barber and Ursell (not generally available) gives rise to errors in the indicated vector components of response. The following analysis for a single-degree-of-freedom system is presented to show the nature and approximate magnitude of such errors due to lag of the averaging device.

The equation of motion of a single-degree-of-freedom system driven by a sinusoidal input of slowly varying frequency is

$$\ddot{y} + 2\zeta\omega_n\dot{y} + y = y_{st}e^{-i\int\omega(t)dt} \tag{A1}$$

The real and imaginary vector components of the response $y(t)$ are determined by averaging the products

$$y(t)\cos\int\omega(t)dt \tag{A2}$$

$$y(t)\sin\int\omega(t)dt \tag{A3}$$

Assume that the products are averaged by devices which have the transfer function of a first-order low-pass filter. In operational form the ratio of output to input for such a filter is

$$\frac{O(s)}{I(s)} = \frac{1}{1 + \tau s} \tag{A4}$$

where τ is the filter time constant and s the Laplace operator.

For the present purpose, assume that the mean values of the products (eqs. (A2) and (A3)) vary with frequency in the same manner as with steady-state excitation at constant frequency.

From the solution of equation (A1) based on steady-state considerations, the real and imaginary vector components are

$$\left[\frac{y(i\omega)}{y_{st}}\right]_R = \frac{1 - \left(\frac{\omega}{\omega_n}\right)^2}{\left[1 - \left(\frac{\omega}{\omega_n}\right)^2\right]^2 + \left(2\zeta \frac{\omega}{\omega_n}\right)^2} \tag{A5}$$

$$\left[\frac{y(i\omega)}{y_{st}}\right]_I = \frac{-2\zeta\left(\frac{\omega}{\omega_n}\right)}{\left[1 - \left(\frac{\omega}{\omega_n}\right)^2\right]^2 + \left(2\zeta \frac{\omega}{\omega_n}\right)^2} \tag{A6}$$

These components are plotted in figure 18 against ω/ω_n for the case $\zeta = 0.05$. Note that near resonance $\left(\frac{\omega}{\omega_n} \approx 1.0\right)$, the major contribution of response comes from the imaginary component.

Let the frequency vary linearly with time such that

$$\omega(t) = \omega_n + \dot{\omega}t$$

or measured from ω_n

$$\omega(t) - \omega_n = \dot{\omega}t \tag{A7}$$

A convenient nondimensional parameter is obtained by dividing equation (A7) by the half-power bandwidth of the system $(\delta = 2\zeta\omega_n)$ to give

$$\left.\begin{aligned} \frac{\dot{\omega}t}{\delta} &= \frac{\omega(t) - \omega_n}{2\zeta\omega_n} \\ \frac{t}{t_b} &= \frac{1}{2\zeta}\left(\frac{\omega}{\omega_n} - 1\right) \end{aligned}\right\} \tag{A8}$$

where $t_b = \frac{\delta}{\dot{\omega}}$ is the time required for the input frequency to sweep through one bandwidth. The ratio t/t_b is also shown as an abscissa in figure 18. The advantage in using this particular nondimensional ratio is that it combines the sweep rate of the input and the parameters of the system into a single variable. The following functions were found to be suitable approximations of the real and imaginary vector components,

$$\left.\begin{aligned}\left[\frac{y(i\omega)}{y_{st}}\right]_R &= -\frac{1}{4\zeta}\sin\left(\pi\frac{t}{t_b}\right)\\ \left[\frac{y(i\omega)}{y_{st}}\right]_I &= -\frac{1}{4\zeta}\left[1+\cos\left(\pi\frac{t}{t_b}\right)\right]\end{aligned}\right\} \tag{A9}$$

and are indicated by the dashed curves in figure 18.

With the inputs to the filters expressed by equations (A9) the outputs, transients being neglected, are found to be

$$\left.\begin{aligned}O\left(\frac{t}{t_b}\right)_R &= -\frac{1}{4\zeta}\frac{\sin\left(\pi\frac{t}{t_b}-\psi\right)}{\sqrt{1+\left(\pi\frac{\tau}{t_b}\right)^2}}\\ O\left(\frac{t}{t_b}\right)_I &= -\frac{1}{4\zeta}\left[1+\frac{\cos\left(\pi\frac{t}{t_b}-\psi\right)}{\sqrt{1+\left(\pi\frac{\tau}{t_b}\right)^2}}\right]\end{aligned}\right\} \tag{A10}$$

where

$$\psi = \tan^{-1}\pi\frac{\tau}{t_b}$$

Consider first the error in maximum response due to filter lag. The maximum value of the imaginary component is a close approximation to the maximum response

$$O_{max} = \frac{1}{4\zeta}\left[1 + \frac{1}{\sqrt{1 + \left(\pi \frac{\tau}{t_b}\right)^2}}\right] \tag{A11}$$

This is to be compared with the true maximum steady-state response of the system which for small damping ($\zeta \ll 1.0$) is from equation (A6)

$$\left|\frac{y(i\omega)}{y_{st}}\right|_{I,max} = \frac{1}{2\zeta} \tag{A12}$$

Thus from equations (A6), (A11), and (A12) the error in maximum response due to filter lag relative to the steady-state maximum may be expressed as

$$\left.\begin{aligned} \frac{\Delta y_\tau}{y(i\omega)_{I,max}} &= \frac{\left[\frac{y(i\omega)}{y_{st}}\right]_{I,max} - O_{max}}{\left[\frac{y(i\omega)}{y_{st}}\right]_{I,max}} \\ \frac{\Delta y_\tau}{y(i\omega)_{I,max}} &= \frac{1}{2}\left[1 - \frac{1}{\sqrt{1 + \left(\pi \frac{\tau}{t_b}\right)^2}}\right] \end{aligned}\right\} \tag{A13}$$

A plot of this error against τ/t_b is shown in figure 3(b).

The second error of interest is the shift in the frequency of maximum response. From equation (A10) it is seen that the filter output reaches a maximum value at a time

$$t_{max} = \frac{t_b \Psi}{\pi} = \frac{t_b}{\pi} \tan^{-1} \pi \frac{\tau}{t_b} \tag{A14}$$

after the input frequency passes through resonance. Therefore, the indicated resonant frequency is shifted by an amount $\dot{\omega} t_m$ from the steady-state resonant frequency. Expressed in bandwidths the resonant frequency shift is

$$\frac{\Delta\omega_\tau}{\delta} = \frac{t_m}{t_b} = \frac{1}{\pi}\tan^{-1}\left(\frac{\pi t}{t_b}\right) \tag{A15}$$

This relation is also plotted in figure 3(b). A comparison between the predicted errors and those determined from analog-computer results (data points in figure) indicates good agreement despite the approximate nature of the analysis.

A third error which can readily be evaluated is the frequency-response phase-angle shift associated with filter lag. The true phase angle is by equations (A5) and (A6)

$$\left.\begin{aligned}\varphi_{true} &= \tan^{-1}\left[\frac{y(i\omega)_I}{y(i\omega)_R}\right] \\ \varphi_{true} &= \tan^{-1}\left[\frac{-2\zeta\,\frac{\omega}{\omega_n}}{1 - \left(\frac{\omega}{\omega_n}\right)^2}\right]\end{aligned}\right\} \tag{A16}$$

The indicated phase angle is $-\frac{\pi}{2}$ when the real component given by equation (A10) passes through zero. This occurs when $t = \tau$ or, in terms of frequency, when

$$\left.\begin{aligned}\frac{\omega}{\omega_n} &= 1 + \frac{\dot{\omega}\tau}{\omega_n} \\ \frac{\omega}{\omega_n} &= 1 + 2\zeta\,\frac{\tau}{t_b}\end{aligned}\right\} \tag{A17}$$

The true phase angle at this frequency is

$$\varphi_{true} = \tan^{-1}\frac{-2\zeta\left(1 + 2\zeta\,\frac{\tau}{t_b}\right)}{1 - \left(1 + 2\zeta\,\frac{\tau}{t_b}\right)^2} \tag{A18}$$

When ζ and τ/t_b are small relative to unity, equation (A18) becomes

$$\varphi_{true} \approx \frac{\pi}{2} - \frac{2\tau}{t_b}$$

Therefore, in the vicinity of resonance, the phase-angle error due to filter lag is

$$\left.\begin{aligned} \Delta\varphi &= \varphi_{true} - \varphi_{indicated} \\ \Delta\varphi &= -\frac{2\tau}{t_b} \end{aligned}\right\} \qquad \text{(A19)}$$

APPENDIX B

FREQUENCY-SWEEP INPUTS DESIGNED TO PRODUCE UNIFORM FREQUENCY SPECTRA

The problem considered is that of controlling the sweep rate of a constant-amplitude variable-frequency time function $P(t)$ such that in the frequency plane its Fourier transform $\left|F\left[P(t)\right]\right|$ is approximately uniform over the band of frequencies covered by the sweep. (See sketch a.)

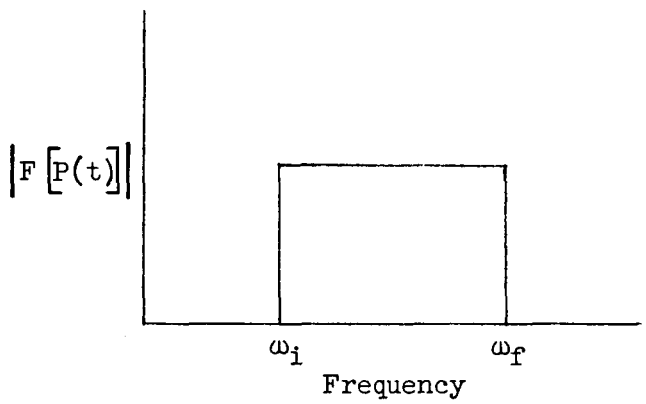

Sketch (a).- Desired uniform frequency spectrum.

Although there are many possible forms of the function $P(t)$ which could be tailored to produce an approximate uniform spectrum, the present analysis will consider as typical examples those functions shown in sketch (b).

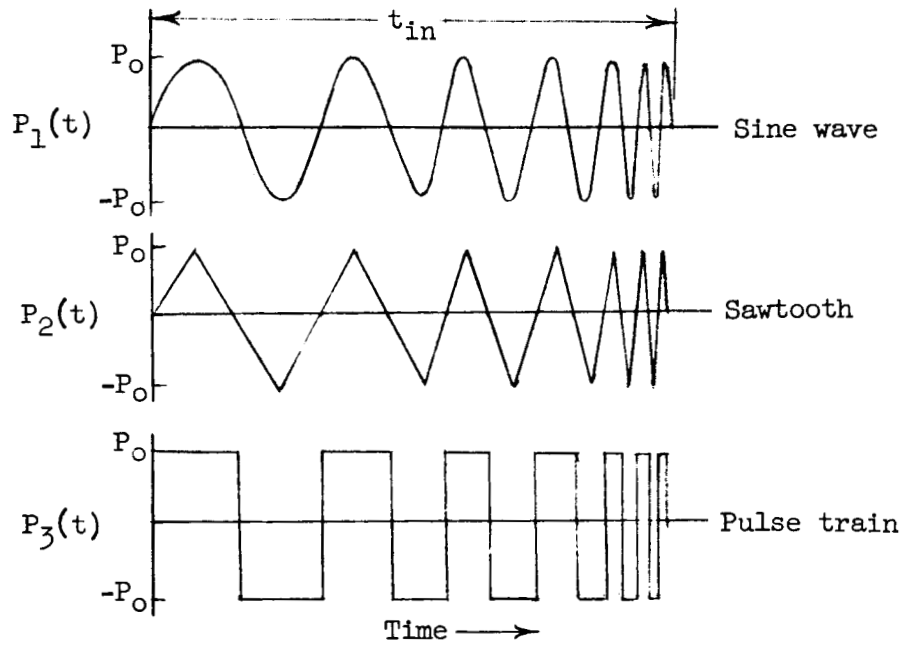

Sketch (b).- Time histories of transient forcing functions.

It is assumed that in the time duration t_{in} over which the forcing function acts, the "instantaneous" fundamental frequency varies continuously from an initial value ω_i to a final value ω_f. The aim of the present analysis is first to find the form of the variation of ω with time required to generate a uniform spectrum, and second to estimate the level of the spectrum.

First consider the sine wave of variable frequency shown at the top of sketch (b). The equation for this function is

$$\left.\begin{aligned} P_1(t) &= P_o \sin \int_0^t \omega(t)\, dt \qquad (0 < t < t_f) \\ P_1(t) &= 0 \qquad (t < 0 \quad \text{and} \quad t > t_f) \end{aligned}\right\} \tag{B1}$$

Assume that the variation of $\omega(t)$ with time is sufficiently slow that over an interval Δt equation (B1) may be approximated by a sine wave of constant frequency

$$P_1(t) \approx P_o \sin \omega_1 t \qquad (t_1 < t < t_1 + \Delta t) \tag{B2}$$

where ω_1 is the average frequency over the interval Δt. The total energy contained in $P_1(t)$ over this interval can be expressed as

$$\int_{t_1}^{t_1+\Delta t} P_1^2(t)dt = P_o^2 \int_0^{\Delta t} \sin^2\omega_1 t \, dt \tag{B3}$$

If $P_1(t)$ undergoes n oscillations in time Δt such that

$$n = \frac{\omega_1 \Delta t}{2\pi}$$

(n = integer), the integration of equation (B3) gives

$$P_o^2 \int_0^{\Delta t} \sin \omega_1 t \, dt = \frac{P_o^2 \Delta t}{2} \tag{B4}$$

The assumption of n being an integer was made in order to simplify equation (B4). The effects of n being other than an integer become negligible as n increases. Equation (B4) shows that the total energy in $P_1(t)$ is simply proportional to the duration of Δt and is independent of frequency. In order to achieve a uniform spectrum, it is required that the energy per $\Delta\omega$ ($\Delta\omega$ being the frequency increment in Δt seconds) remain constant over the frequency band covered by the sweep. Thus, when equation (B4) is divided by $\Delta\omega$ and the result is set equal to a constant, it is seen that the ratio $\Delta\omega/\Delta t$ must be held constant during the sweep; that is, a linear variation of frequency with time is required to produce a uniform spectrum.

The second point of interest is the relationship between the level of the spectrum and the frequency-sweep rate. Parseval's theorem, which relates the total energy of an arbitrary time function to the area under the square of its frequency spectrum, provides the basis of finding an effective spectrum level.

Parseval's theorem for Fourier integrals states

$$\left.\begin{aligned} \int_{-\infty}^{\infty} P^2(t)dt &= \frac{1}{2\pi} \int_{-\infty}^{\infty} \left|F\left[P(t)\right]\right|^2 d\omega \\ \int_{-\infty}^{\infty} P^2(t)dt &= \frac{1}{\pi} \int_{0}^{\infty} \left|F\left[P(t)\right]\right|^2 d\omega \end{aligned}\right\} \tag{B5}$$

The left-hand side of equation (B5) for the case of a variable-frequency sine wave has been shown to depend only on the time over which $P_1(t)$ acts and not on the frequency (see eq. (B4)); therefore,

$$\int_{-\infty}^{\infty} P_1^2(t)dt = \frac{P_o^2 t_{in}}{2} \tag{B6}$$

Since the shape of the frequency spectrum is assumed to be rectangular, the right-hand side of the equation may be defined as the product of an "effective" spectrum height times the frequency band covered in the sweep.

$$\frac{1}{\pi} \int_0^{\infty} \left|F\left[P_1(t)\right]\right|^2 d\omega = \left|F\left[P_1(t)\right]\right|_{eff}^2 (\omega_f - \omega_i) \tag{B7}$$

When equation (B6) is equated to (B7), the effective spectrum level is found to be

$$\left.\begin{aligned} \left|F\left[P_1(t)\right]\right|_{eff} &= \frac{\sqrt{\frac{\pi}{2}}\, P_o}{\left(\frac{\omega_f - \omega_i}{t_{in}}\right)^{1/2}} \\ \left|F\left[P_1(t)\right]\right| &= \sqrt{\frac{\pi}{2}} \frac{P_o}{\sqrt{\dot{\omega}}} \end{aligned}\right\} \tag{B8}$$

By a similar procedure the effective spectrum level of the two other functions shown in sketch (b) are:

For the sawtooth function:

$$\left|F\left[P_2(t)\right]\right|_{eff} = \sqrt{\frac{\pi}{3}} \frac{P_o}{\sqrt{\dot{\omega}}} \tag{B9}$$

and for the pulse train:

$$\left|F\left[P_3(t)\right]\right|_{eff} = \sqrt{\pi} \frac{P_o}{\sqrt{\dot{\omega}}} \tag{B10}$$

As stated previously, this analysis is based on the assumption that the variation of $\omega(t)$ is sufficiently slow for it to be approximated by a series of constant-frequency intervals. Experience has indicated that this is not a severe assumption. The spectrum level of sweep inputs as rapid as that shown in figure 12(b) can be estimated with reasonable accuracy by equation (B8).

It is interesting to note that of the three functions considered the pulse train not only is richest in frequency content but also would be the simplest to generate in many practical applications.

APPENDIX C

EQUATIONS OF MOTION FOR THE SIMULATED AEROELASTIC SYSTEM

The equations of motion for the vertical translation and torsion degrees of freedom for the airfoil shown in figure 7 are:

$$\left.\begin{aligned} m\ddot{h} + S_\alpha\ddot{\alpha} + C_h h &= l + P(t) \\ I_\alpha\ddot{\alpha} + S_\alpha\ddot{h} + C_\alpha\alpha &= m_a - 2bx_o P(t) \end{aligned}\right\} \qquad \text{(C1)}$$

Structural properties of the system are represented by the left-hand side of the equations and the external forces and moments, originating from aerodynamic and wing shaker forces, are on the right-hand side. The aerodynamic forces and moments are from piston theory (ref. 13).

$$\left.\begin{aligned} l &= \frac{-4\rho Ub}{M}\left[\dot{h} + U\alpha + b(1 - 2x_o)\dot{\alpha} + w_T\right] \\ m_a &= \frac{-4\rho Ub}{M}\left\{(1 - 2x_o)\dot{h} + U(1 - 2x_o)\alpha + b\left[\frac{1}{3} + (1 - 2x_o)^2\right]\dot{\alpha} + (1 - 2x_o)w_T\right\} \end{aligned}\right\} \qquad \text{(C2)}$$

where w_T is a random vertical velocity component of air turbulence.

For convenience the equations were put into a nondimensional form by making the following substitutions:

$$\bar{t} = \omega_h t;\quad k_h = \frac{\omega_h b}{U}$$

$$\mu = \frac{m}{\pi\rho b^2};\quad \bar{\omega} = \frac{\omega}{\omega_h}$$

$$\bar{h} = \frac{h}{b};\quad F(t) = \frac{P(t)}{mb\omega_h^2}$$

$$\omega_h^2 = \frac{C_h}{m};\quad \omega_\alpha^2 = \frac{C_\alpha}{I_\alpha}$$

$$r_\alpha^2 = \frac{I_\alpha}{mb^2}$$

L 9 8 5

The final form of the equations of motion used are:

$$\left.\begin{aligned} \bar{h}'' + a_{11}\bar{h}' + \bar{h} + b_{12}\alpha'' + b_{11}\alpha' + b_{10}\alpha &= F(\bar{t}) - N_T \\ a_{22}\bar{h}'' + a_{21}\bar{h}' + \alpha'' + b_{21}\alpha' + b_{20}\alpha &= -C_1 F(\bar{t}) - C_2\left(\frac{w_T}{U}\right) \end{aligned}\right\} \qquad (C3)$$

where

$$a_{11} = \frac{4}{\pi\mu M k_h}$$

$$b_{12} = x_\alpha$$

$$b_{11} = \frac{4(1 - 2x_o)}{\pi\mu M k_h}$$

$$b_{10} = \frac{4}{\pi\mu M k_h^2}$$

$$a_{22} = \frac{x_\alpha}{r_\alpha^2}$$

$$a_{21} = \frac{4(1 - 2x_o)}{\pi\mu M k_h r_\alpha^2}$$

$$b_{21} = \frac{4\left[\frac{1}{3} + (1 - 2x_o)^2\right]}{\pi\mu M k_h r_\alpha^2}$$

$$b_{20} = \left(\frac{\omega_\alpha}{\omega_h}\right)^2 + \frac{4(1 - 2x_o)}{\pi\mu M k_h^2 r_\alpha^2}$$

$$C_1 = \frac{2x_o}{r_\alpha^2}$$

$$C_2 = \frac{4(1 - 2x_o)}{\pi\mu M k_h^2 r_\alpha^2}$$

$$N_T = b_{10}\left(\frac{w_T}{U}\right)$$

$$( )' = \frac{d( )}{d\omega_h t}$$

$$( )'' = \frac{d^2( )}{d(\omega_h t)^2}$$

In terms of h and α the deflection of the leading edge in semichords is

$$z(t) = \bar{h}(t) - 2x_o\alpha(t) \qquad (C4)$$

All results given in this paper are for the following set of conditions (μ is varied in fig. 14)

$M = 2.0$

$k_h = 0.2$

$x_o = 0.5$

$x_\alpha = 0.2$

$\frac{1}{r_\alpha^2} = 4.0$

$\frac{\omega_\alpha}{\omega_h} = 2.0$

$\mu = 20$

$\omega_h = 1.0$ radians/sec (machine time)

REFERENCES

1. Oldenburger, Rufus, ed.: Frequency Response. The Macmillan Company, c.1956.

2. Lees, Sidney: Interpreting Dynamic Measurements of Physical Systems. Trans. ASME, vol. 80, no. 4, May 1958, pp. 833-857.

3. Bratt, J. B., Wight, K. C., and Tilly, V. J.: The Application of a "Wattmeter" Harmonic Analyzer to the Measurement of Aerodynamic Damping for Pitching Oscillations. R. & M. No. 2063, British A.R.C., 1942.

4. Lessing, Henry C., Fryer, Thomas B., and Mead, Merrill H.: A System for Measuring the Dynamic Lateral Stability Derivatives in High-Speed Wind Tunnels. NACA TN 3348, 1954.

5. Cowley, P. E. A.: The Application of an Analog Computer to the Measurement of Process Dynamics. Trans. ASME, vol. 79, no. 4, May 1957, pp. 823-832.

6. Earshen, John J.: A New Method for Measuring Phase and Amplitude Response of Physical Systems Using Bridge-Connected Transducers. Proc. Nat. Electronic Conf. (Chicago, Ill., 1957), vol. XIII, 1957, pp. 943-958.

7. Hok, Gunnar: Response of Linear Resonant Systems to Excitation of a Frequency Varying Linearly With Time. Jour. Appl. Phys., vol. 19, no. 3, Mar. 1948, pp. 242-250.

8. Laverne, Melvin E., and Boksenbom, Aaron S.: Frequency Response of Linear Systems From Transient Data. NACA Rep. 977, 1950. (Supersedes NACA TN 1935.)

9. Huss, Carl R., and Donegan, James J.: Method and Tables for Determining the Time Response to a Unit Impulse From Frequency-Response Data and for Determining the Fourier Transform of a Function of Time. NACA TN 3598, 1956.

10. Eggleston, John M., and Mathews, Charles W.: Application of Several Methods for Determining Transfer Functions and Frequency Response of Aircraft From Flight Data. NACA Rep. 1204, 1954. (Supersedes NACA TN 2997.)

11. Crane, Harold L.: A Manual Frequency Sweep Technique for the Measurement of Airplane Frequency Response. NASA TN D-375, 1960.

12. Ashley, Holt, and Zartarian, Garabed: Piston Theory - A New Aerodynamic Tool for the Aeroelastician. Jour. Aero. Sci., vol. 23, no. 12, Dec. 1956, pp. 1109-1118.

13. Crane, Harold L., and Chilton, Robert G.: Measurements of Atmospheric Turbulence Over a Wide Range of Wavelength for One Meterological Condition. NACA TN 3702, 1956.

14. Kennedy, Charles C., and Pancu, C. D. P.: Use of Vectors in Vibration Measurement and Analysis. Jour. Aero. Sci., vol. 14, no. 11, Nov. 1947, pp. 603-625.

15. Broadbent, E. G.: Vector Plotting as an Indication of the Approach to Flutter. OSR-9-0269, Proc. Flight Flutter Testing Symposium (Washington, D.C.), May 15-16, 1958, pp. 31-40. (Sponsored by Aircraft Ind. Assoc. and AFOSR.)

16. Pines, Samuel: An Elementary Explanation of the Flutter Mechanism. Proc. Nat. Specialists Meeting on Dynamics and Aeroelasticity (Fort Worth, Texas), Inst. Aero. Sci., Nov. 1958, pp. 52-58.

17. Reed, W. H. III: A Flight Investigation of Oscillating Air Forces: Equipment and Technique. OSR-9-0269, Proc. Flight Flutter Testing Symposium (Washington, D.C.), May 15-16, 1958, pp. 41-50. (Sponsored by Aircraft Ind. Assoc. and AFOSR.)

18. Korn, Granino A., and Korn, Theresa M.: Electronic Analog Computers. Second ed., McGraw-Hill Book Co., Inc., 1956.

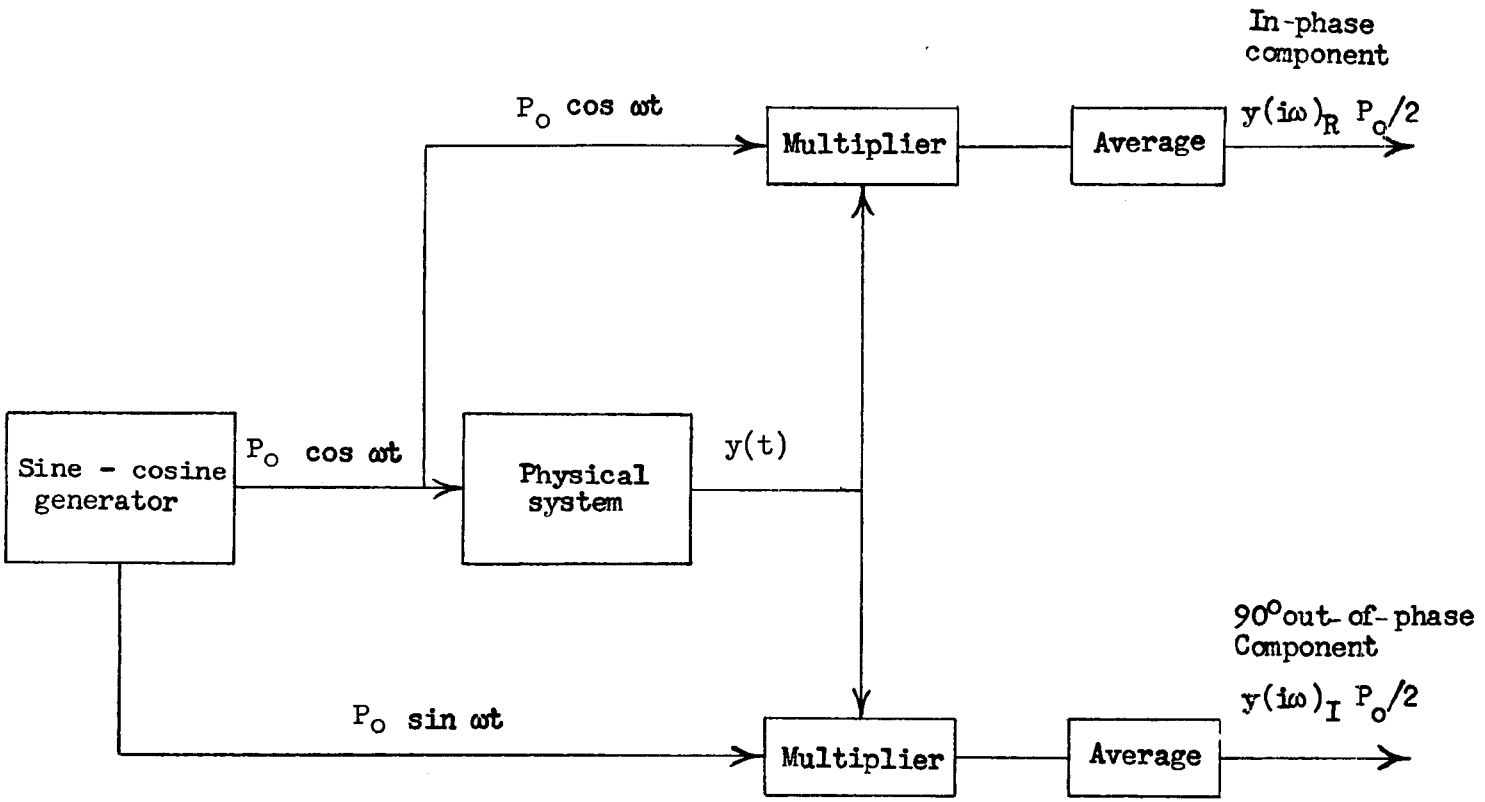

Figure 1.- Wattmeter technique of frequency-response measurements with periodic excitation.

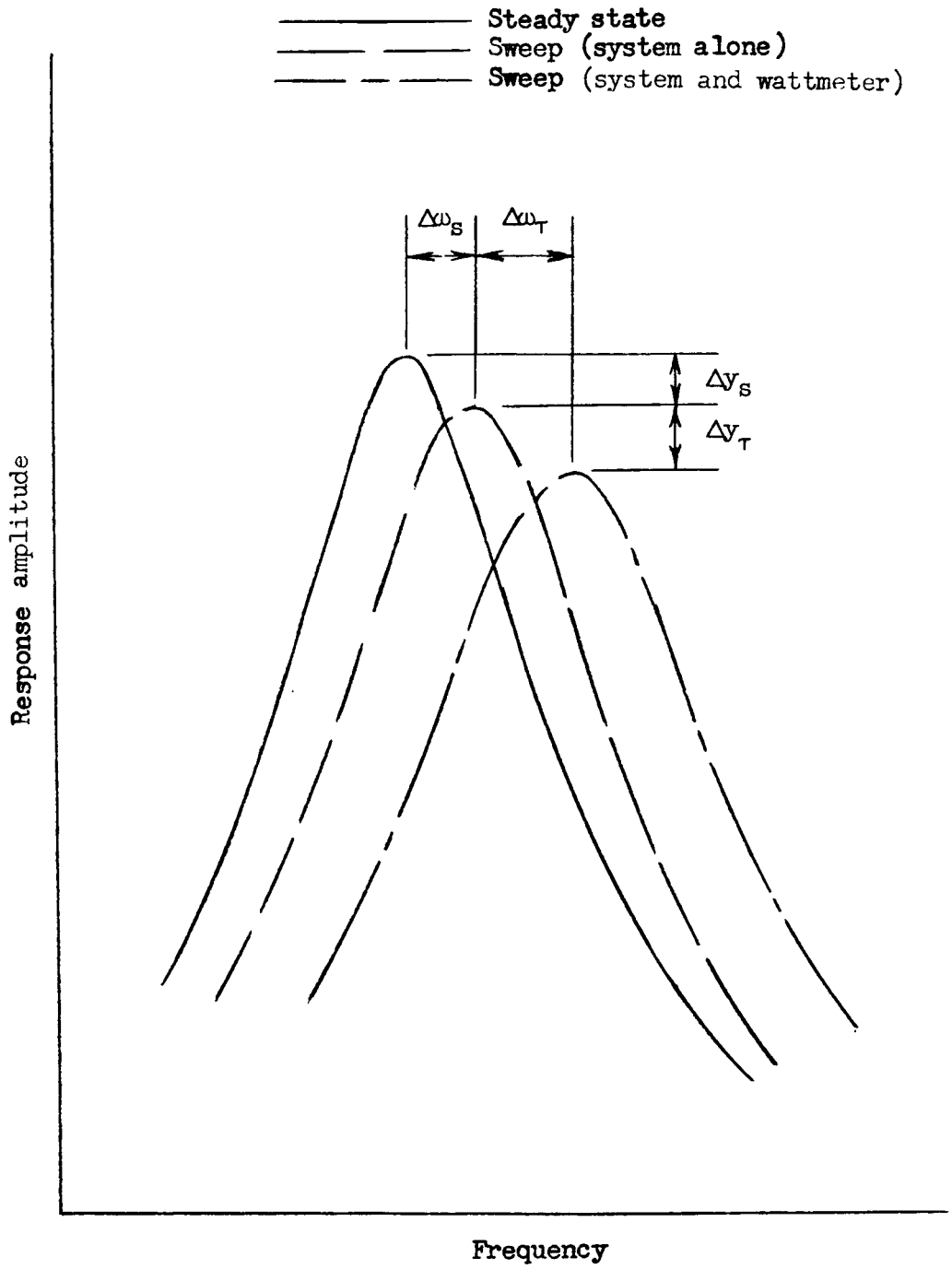

Figure 2.- Illustration of the effects of frequency sweep on the forced response of a system measured by the wattmeter technique.

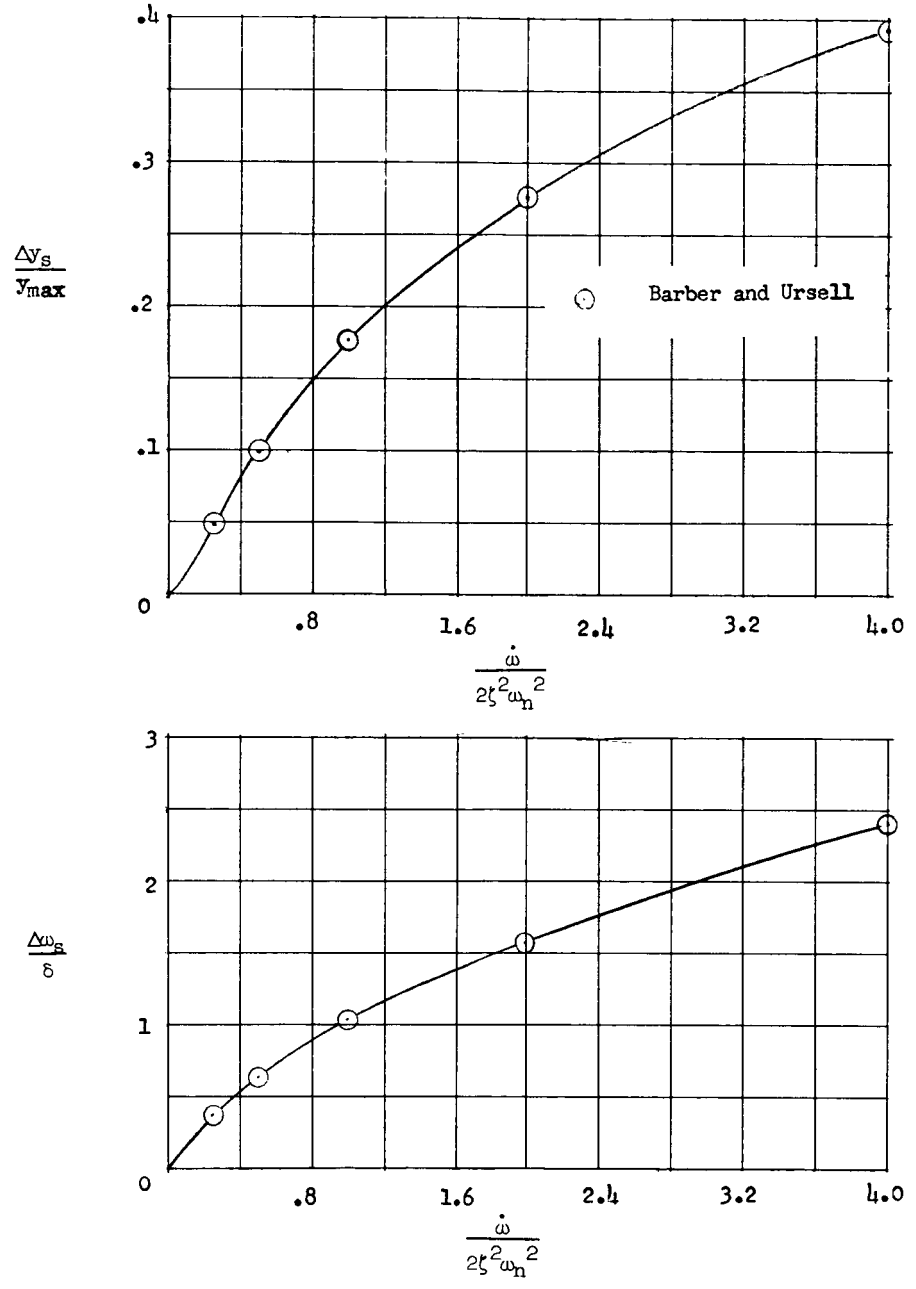

(a) Errors due to sweep alone.

Figure 3.- Errors in frequency and amplitude of maximum response due to frequency sweep.

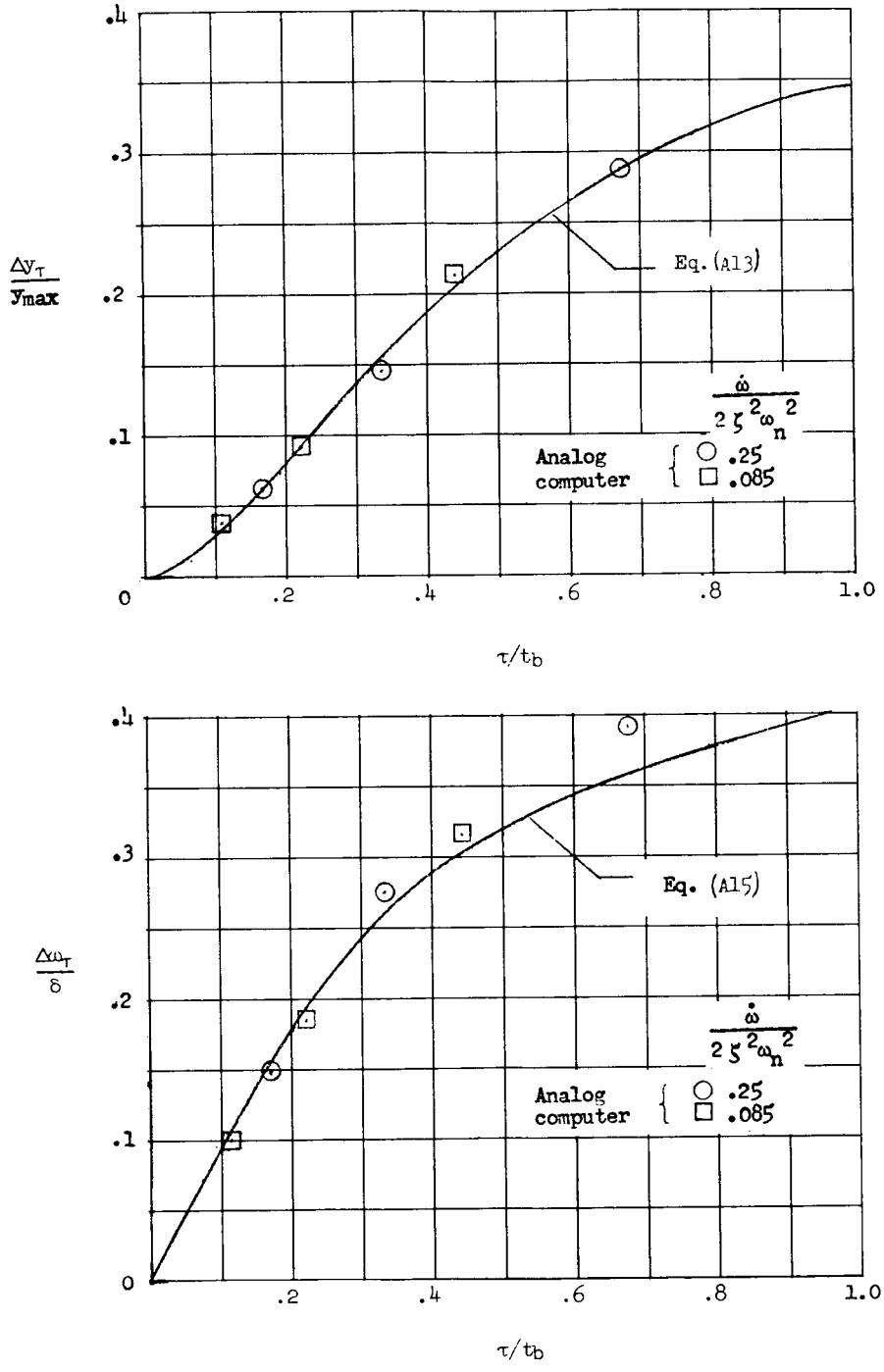

(b) Errors due to lag of averaging device.

Figure 3.- Concluded.

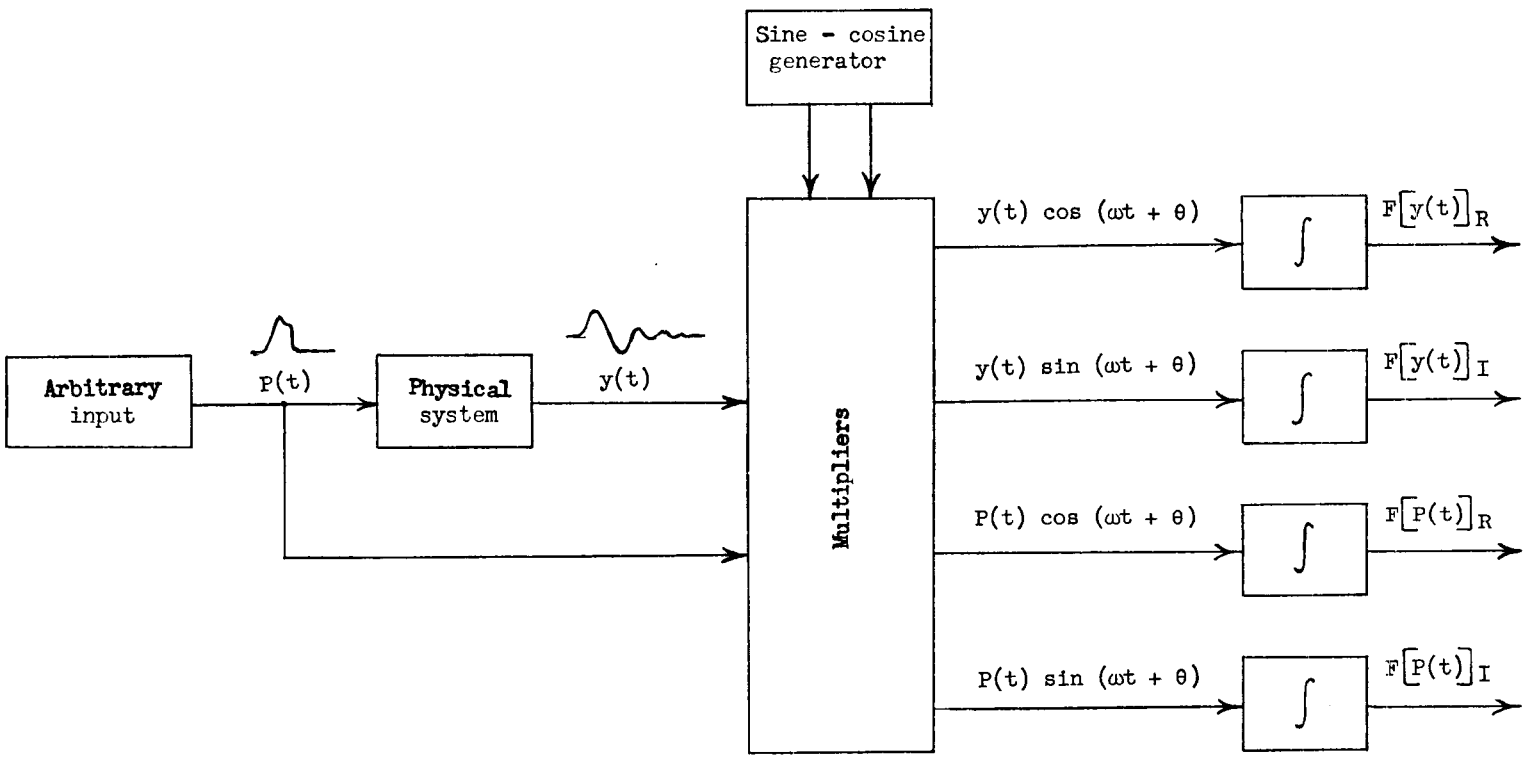

Figure 4.- Technique for frequency-response measurements with arbitrary transient inputs.

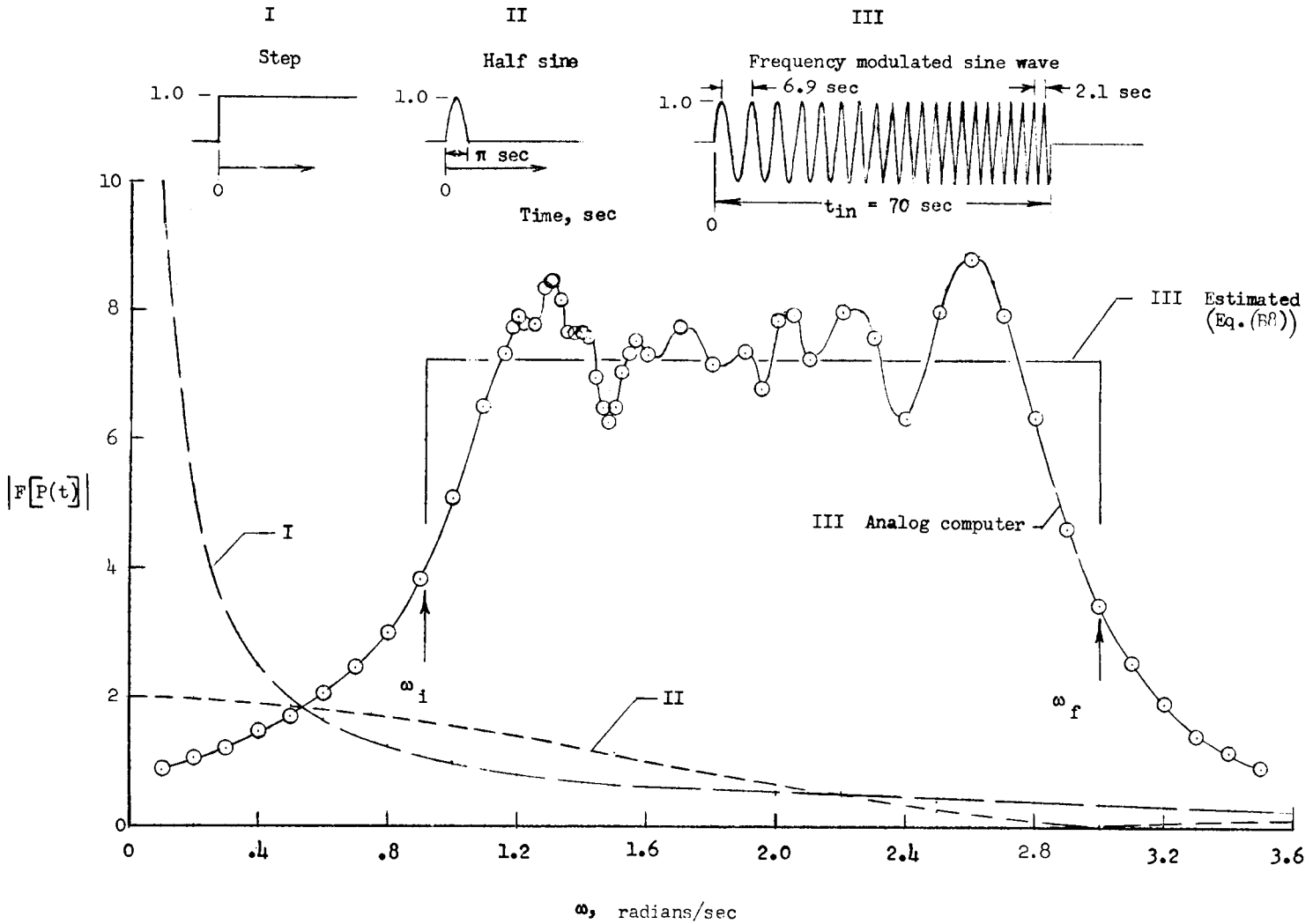

Figure 5.- Comparison of frequency spectra of a step, half-sine wave, and frequency-modulated function.

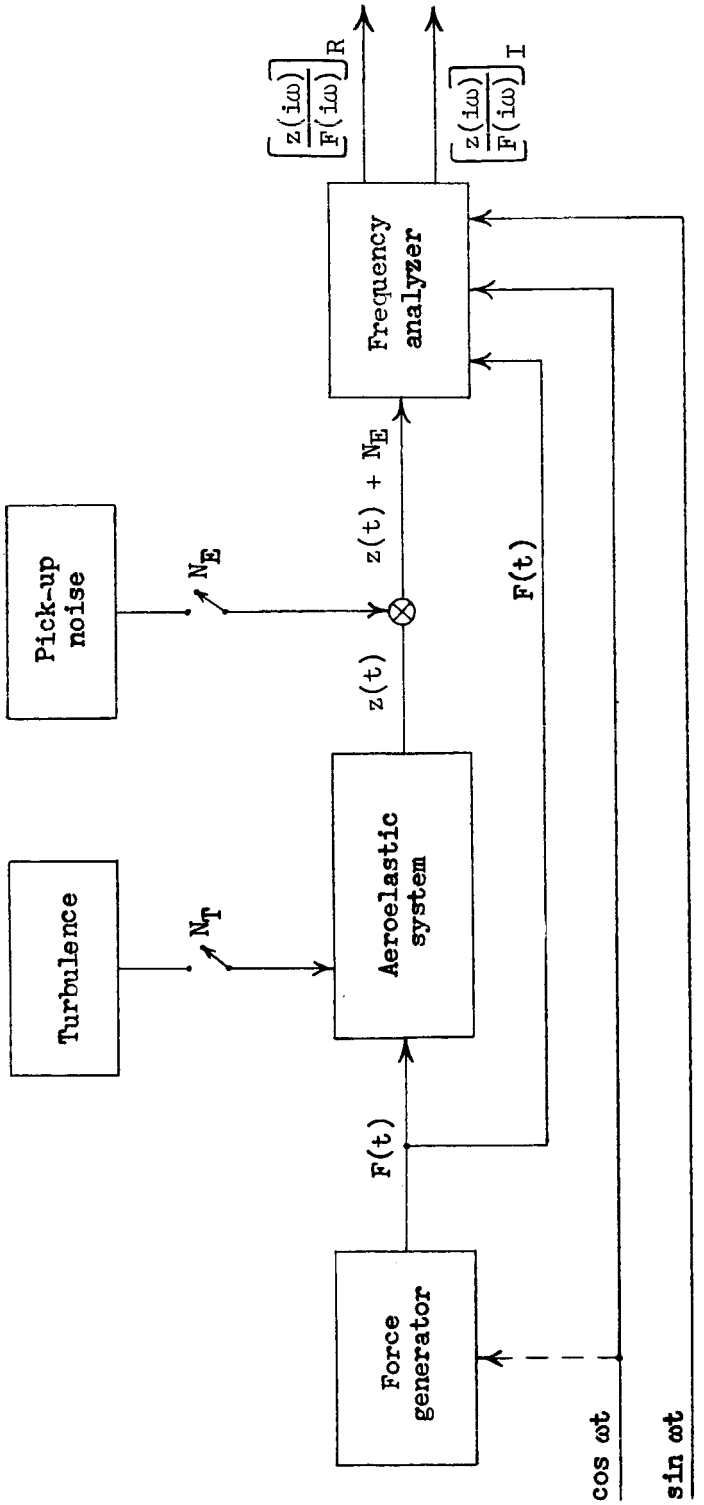

Figure 6.- Analog simulation of a forced aeroelastic response test.

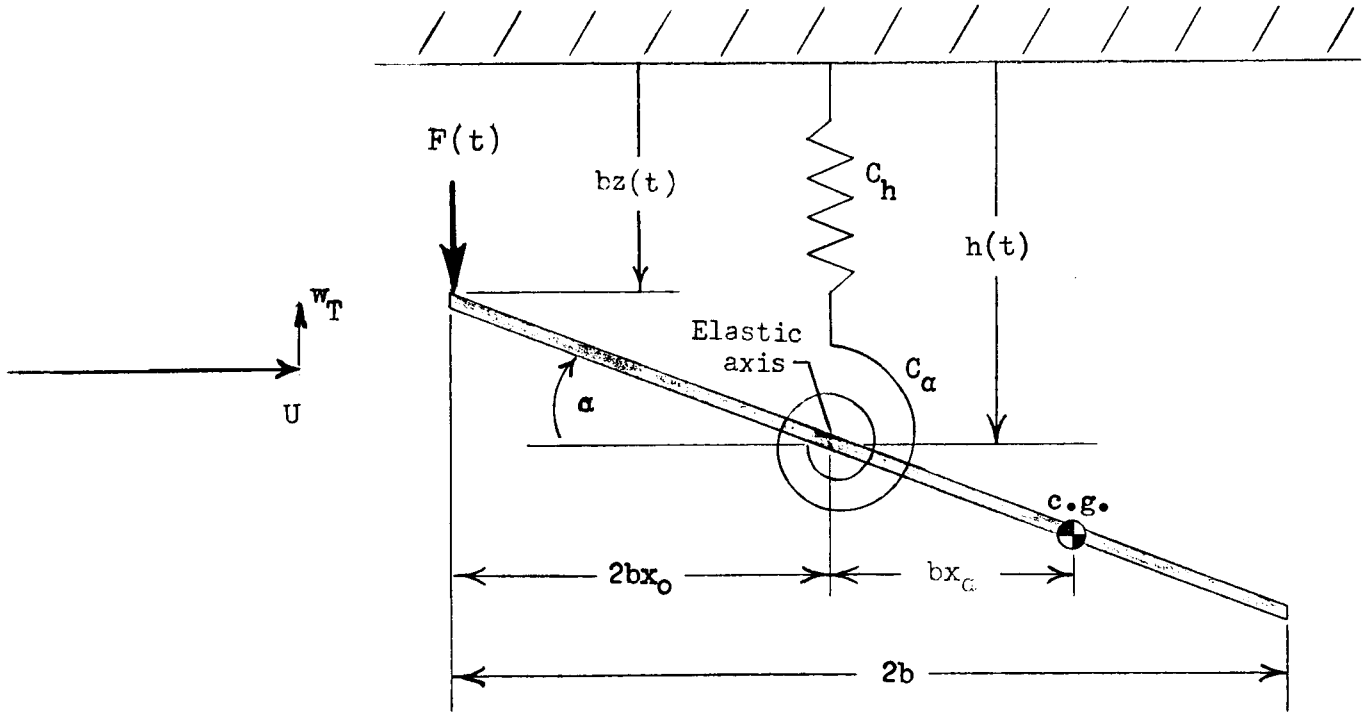

Figure 7.- Schematic diagram of the simulated two-degree-of-freedom aeroelastic system.

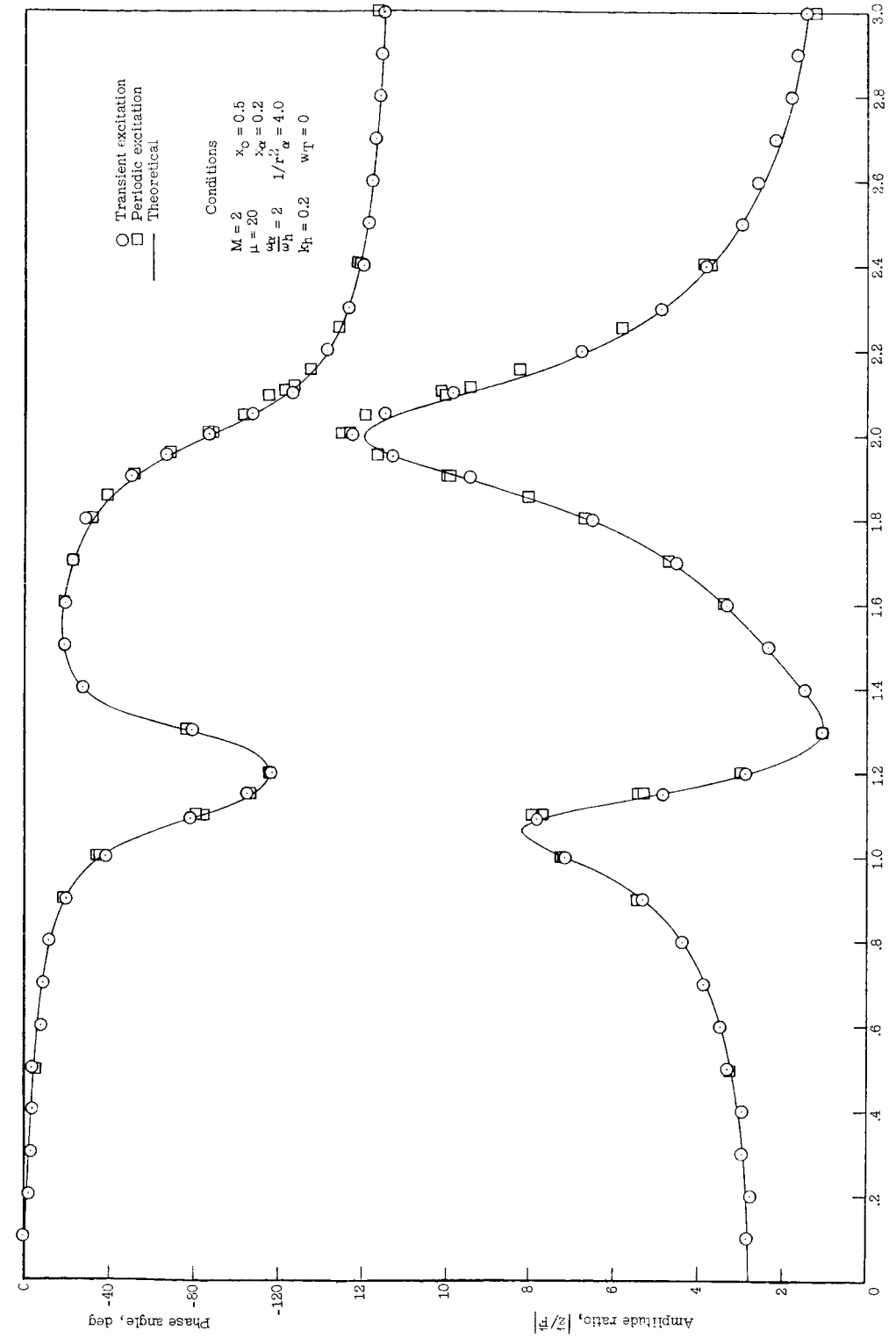

Figure 8.- Frequency response of aeroelastic system determined from the equations of motion and an analog simulation using transient and periodic inputs.

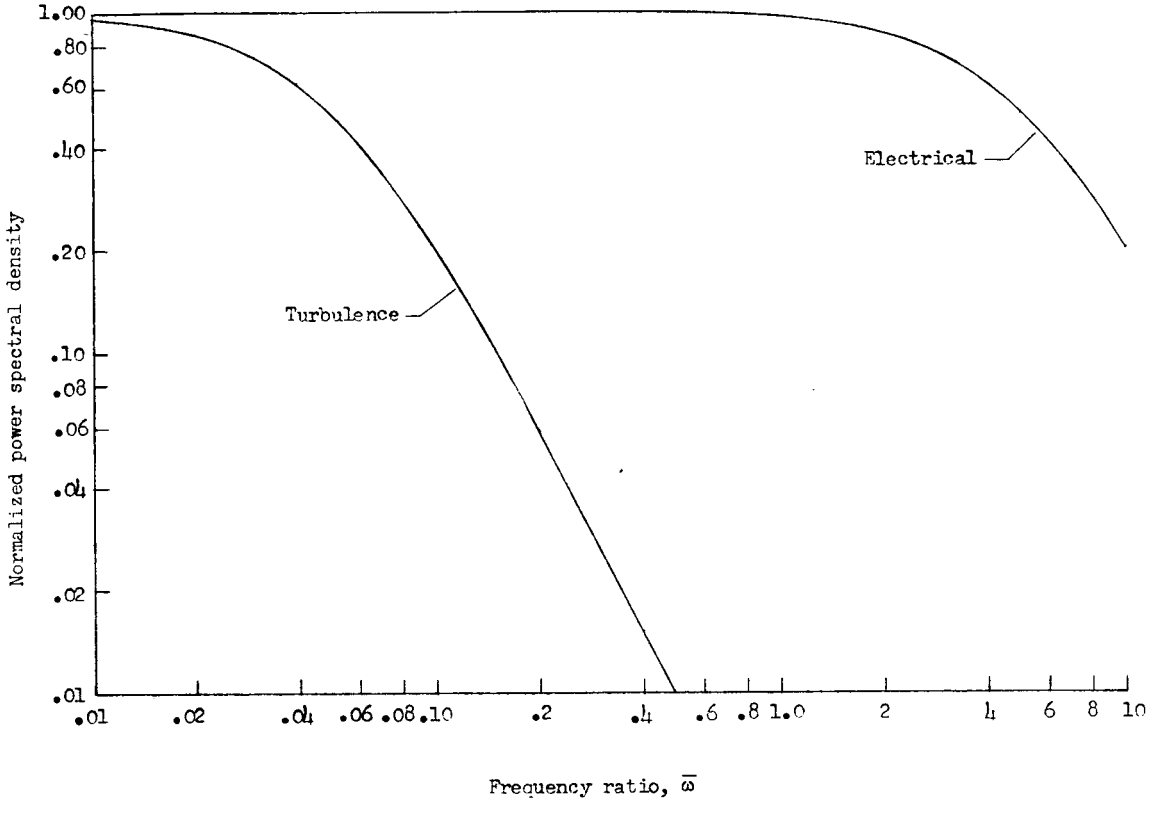

Figure 9.- Power spectral density of simulated atmospheric turbulence and electrical pick-up noise.

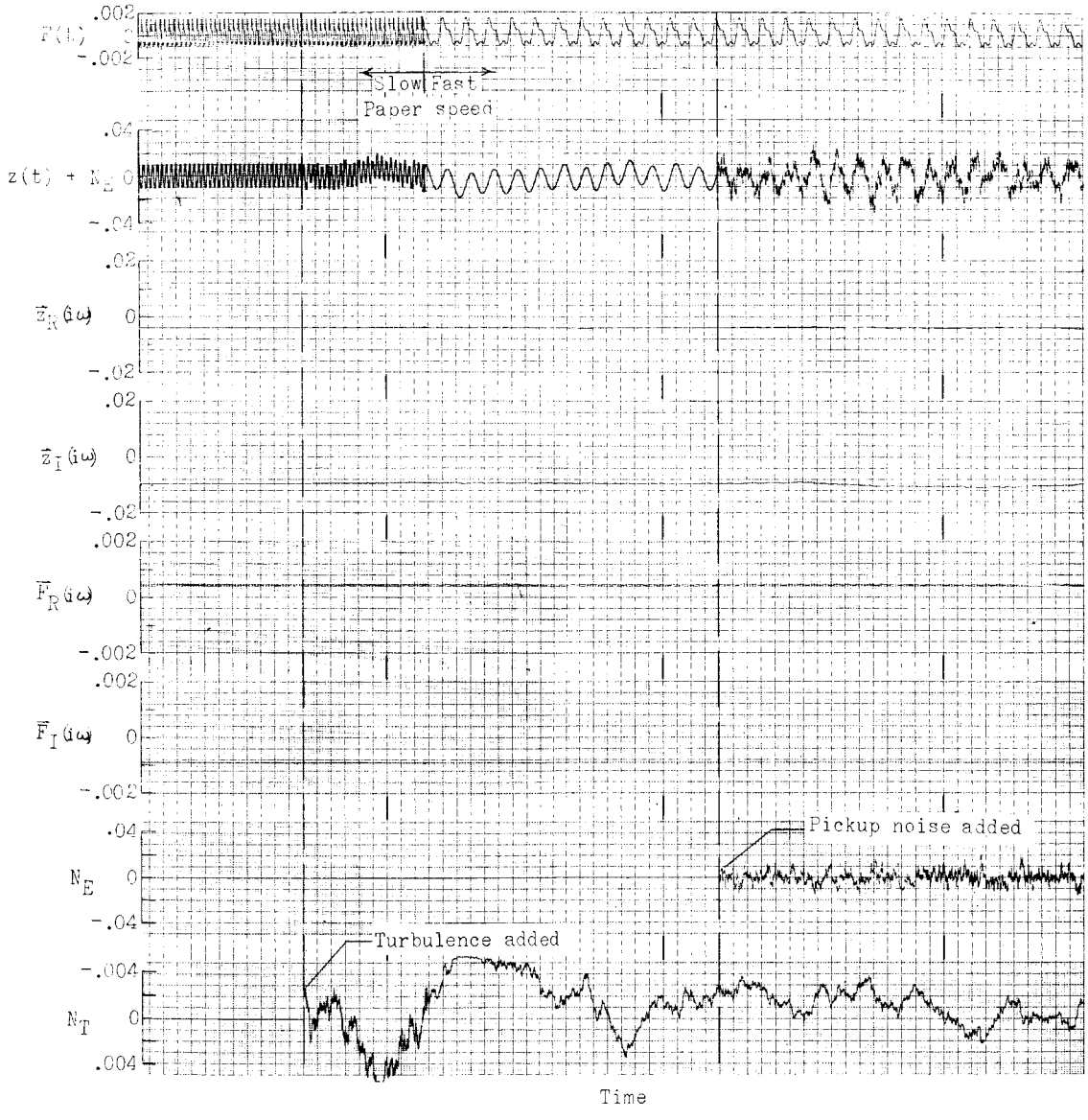

Figure 10.- Periodic forced response of the simulated system illustrating the effects of introducing turbulence and pick-up noise. $\bar{\omega} = 1.9$; $\omega_h T = 40$; $N_T = 0.002$ rms; $N_E = 0.006$ rms.

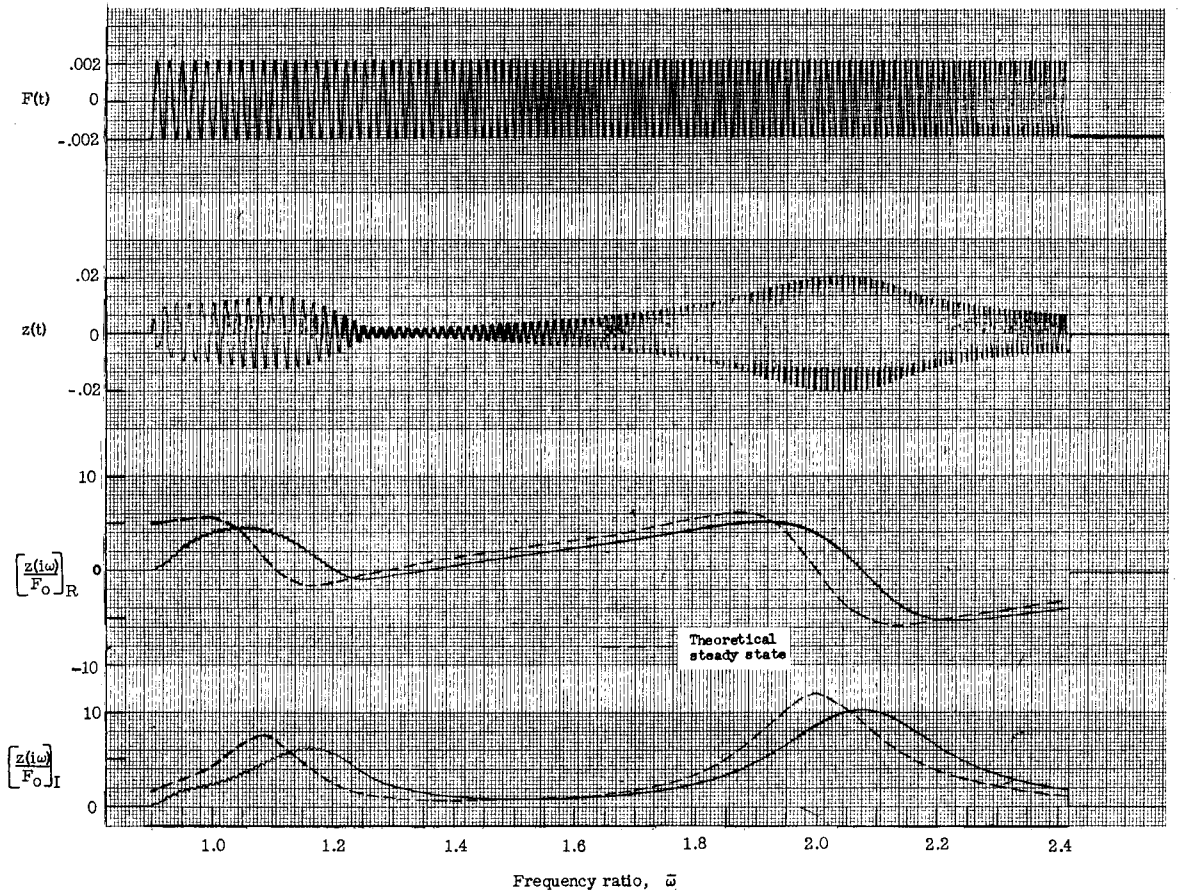

(a) Time histories. (Theoretical steady-state response components are shown for comparison with measured values.)

Figure 11.- Response of the simulated system to a slowly varying excitation frequency. $\frac{\dot{\omega}}{\omega_h^2} = 0.003$; $\omega_h \tau = 20$.

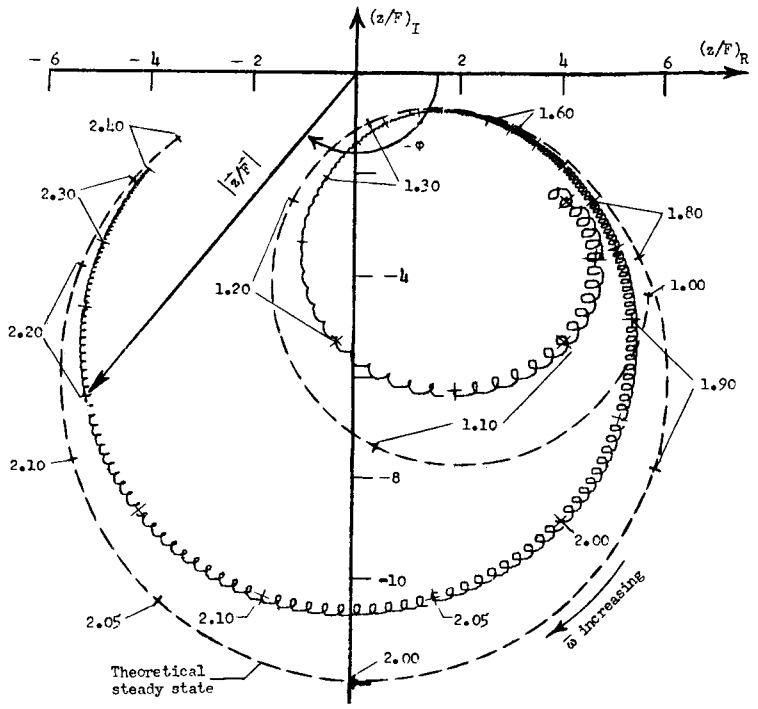

(b) Polar plot. (Theoretical steady-state plot also given.)

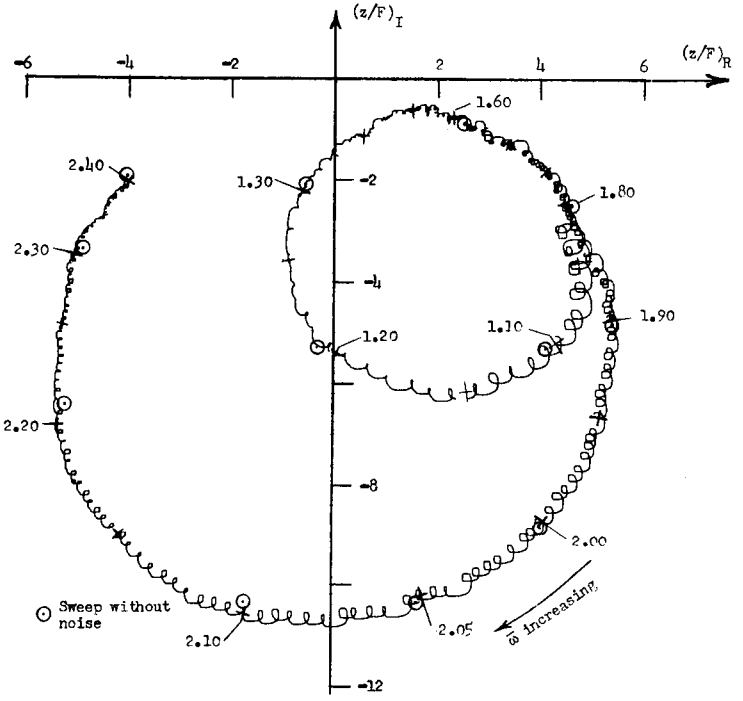

(c) Polar plot made in the presence of noise. (N_T = 0.0013 rms; N_E = 0.0005 rms.)

Figure 11.- Concluded.

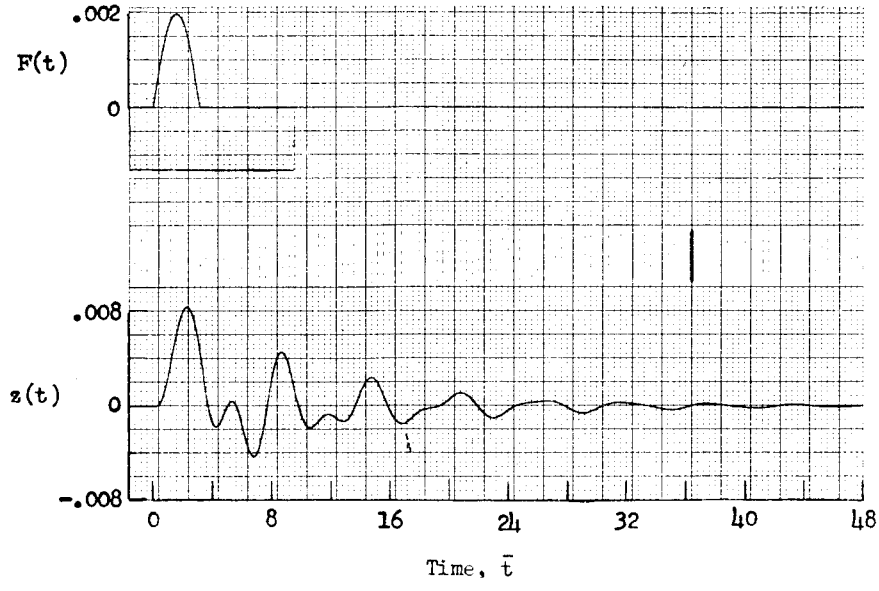

(a) Half-sine wave pulse. $\left(\omega_h t_{in} = \pi.\right)$

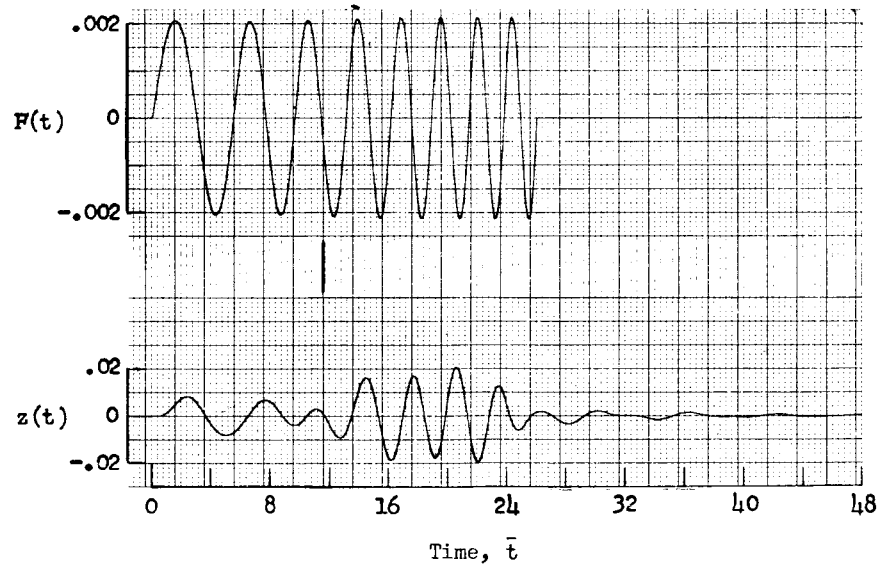

(b) Rapid frequency sweep. $\left(\frac{\omega_i}{\omega_h} = 0.92;\ \frac{\omega_f}{\omega_h} = 3.2.\right)$

Figure 12.- Transient response of the simulated system to a pulse and a rapid frequency-sweep input.

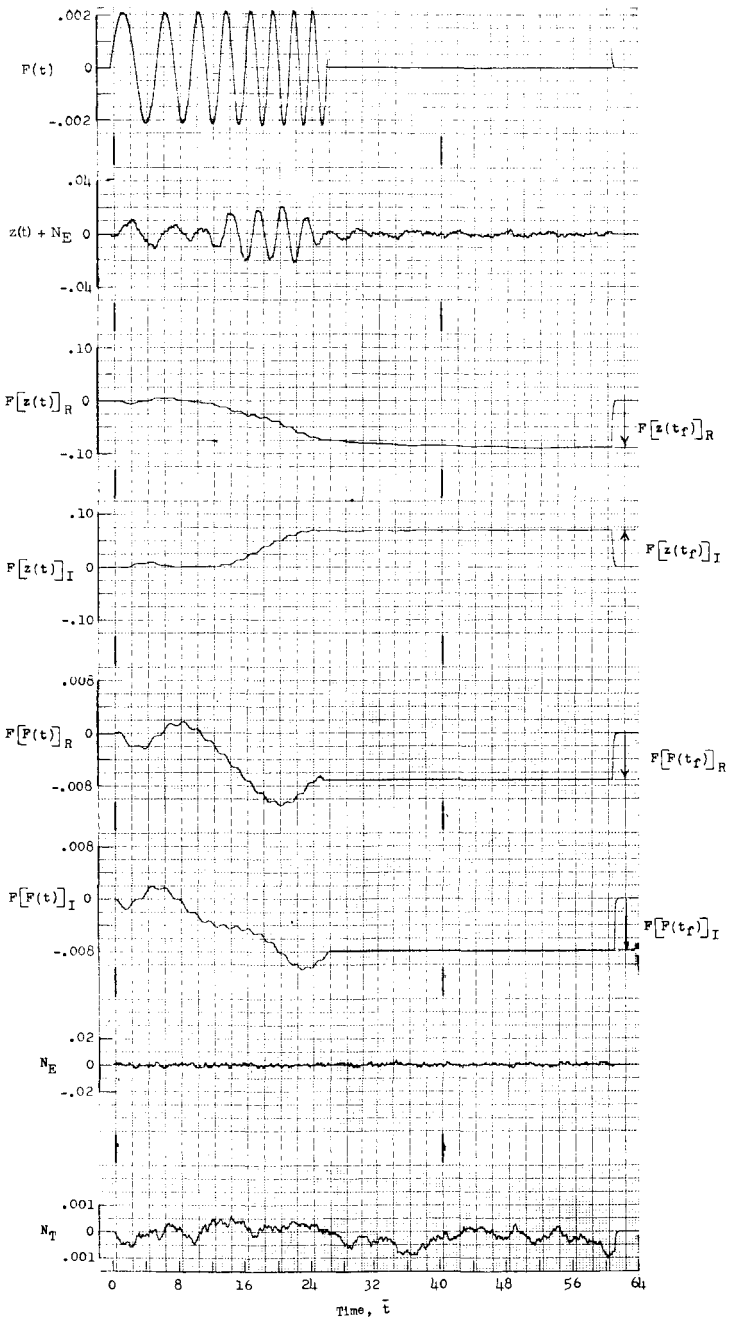

Figure 13.- Evaluation of Fourier transforms at $\frac{\omega}{\omega_h} = 2.0$ for rapid sweep input with random noise added. (Input same as fig. 12(b); $N_T = 0.004$ rms; $N_E = 0.001$ rms.)

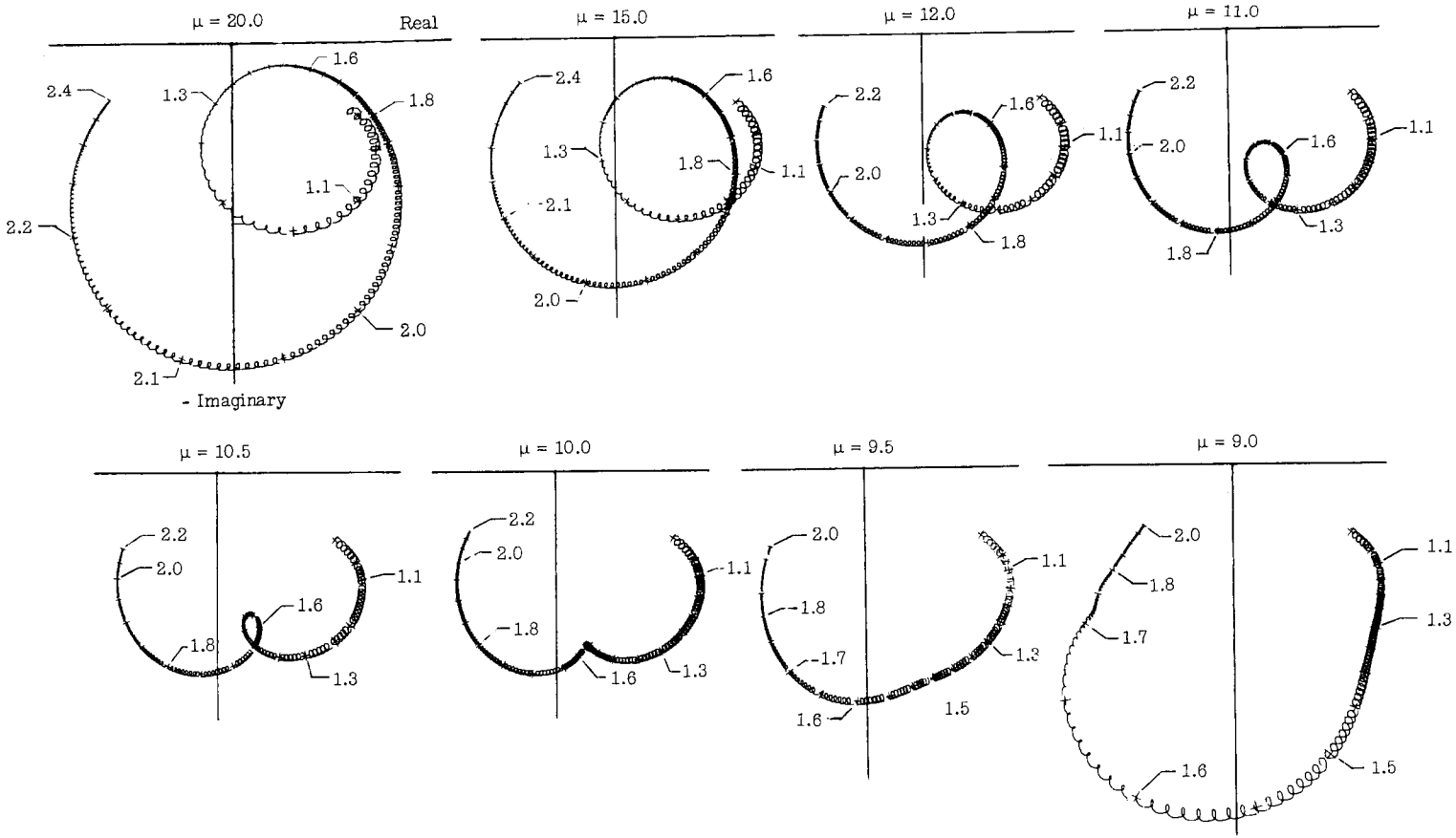

Figure 14.- Polar frequency-response plots showing approach to flutter as density ratio is varied. $\left(\mu_{flutter} = 8.3;\ \frac{\dot{\omega}}{\omega_h^2} = 0.003;\ \omega_h \tau = 20.\right)$

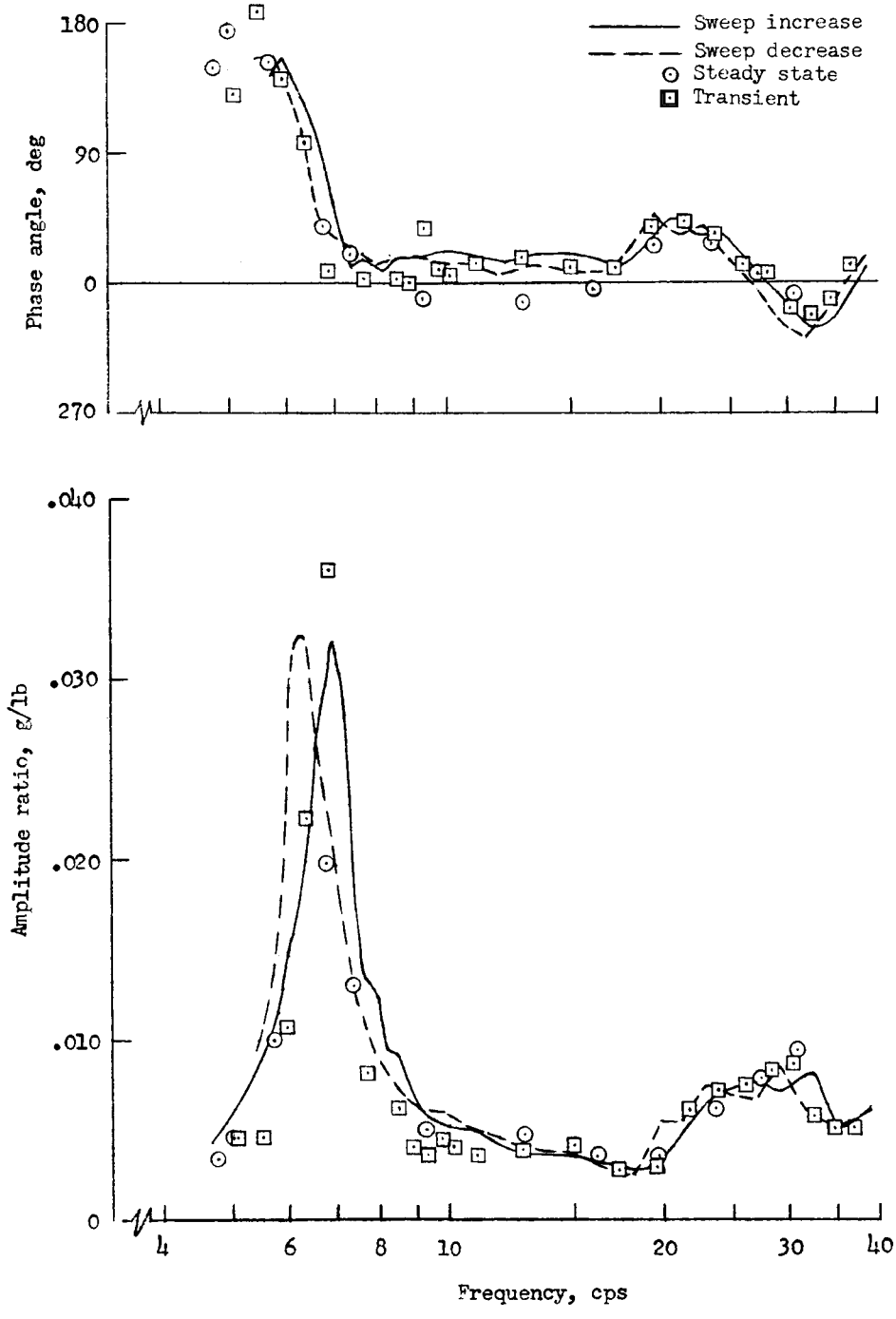

Figure 15.- Wing frequency-response data obtained by three methods of excitation during flight tests at M = 0.83 ± 0.03 and an altitude of 20,000 feet.

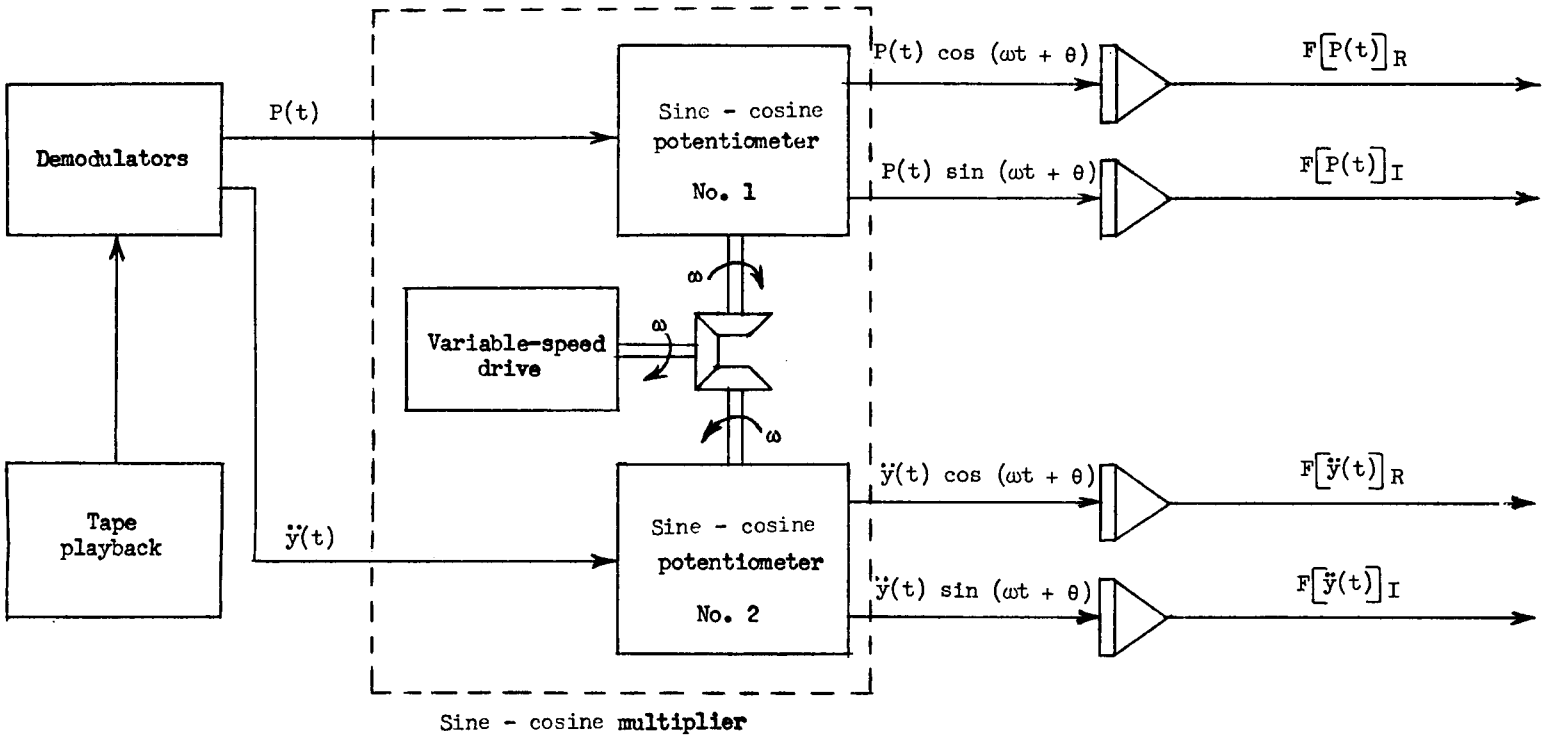

(a) Block diagram of analyzer.

Figure 16.- Analog method of analyzing transient flight-test data.

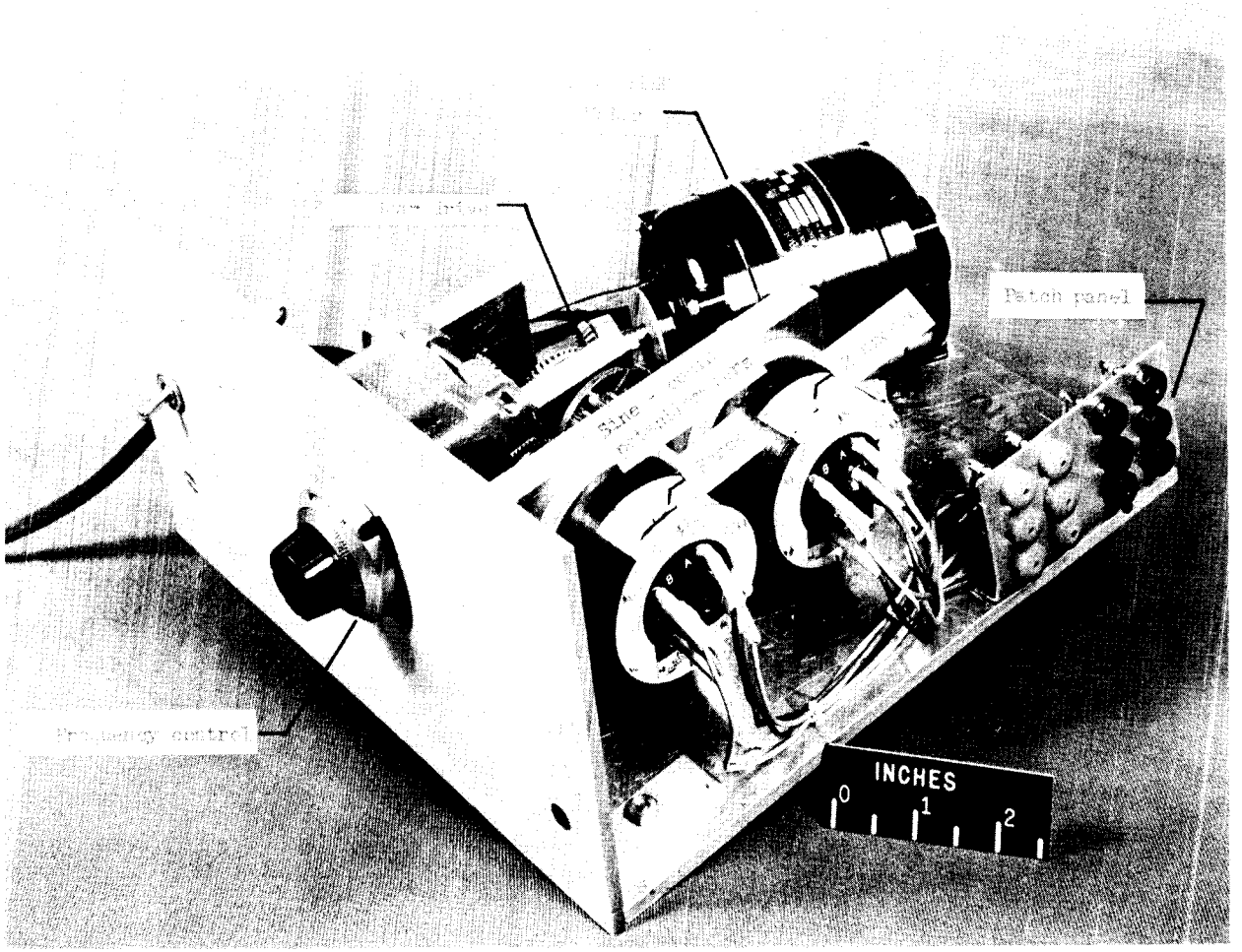

L-59-8267.1

(b) Photograph of mechanically driven sine-cosine potentiometers.

Figure 16.- Concluded.

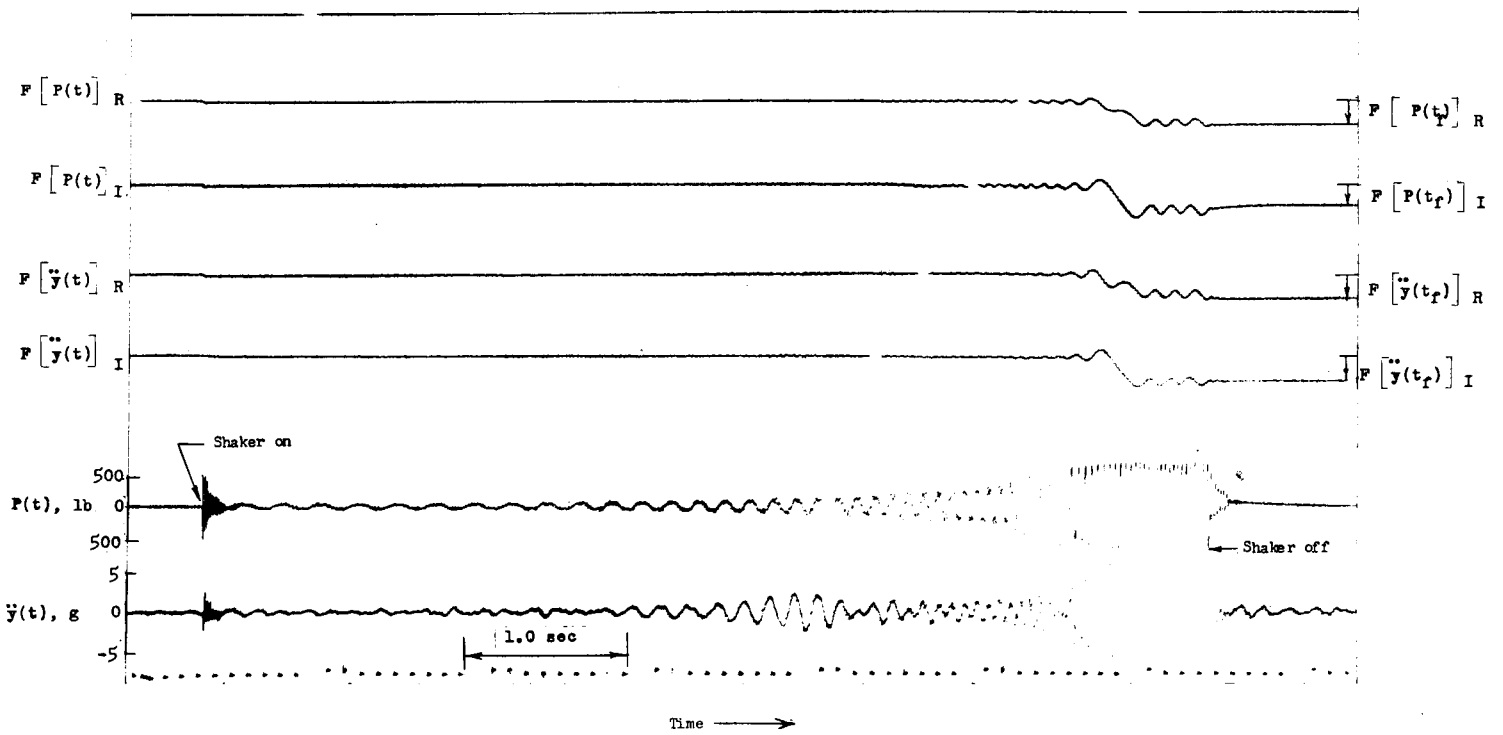

Figure 17.- Sample record showing the transient analysis of rapid sweep data. (Analyzer frequency = 31.2 cps.)

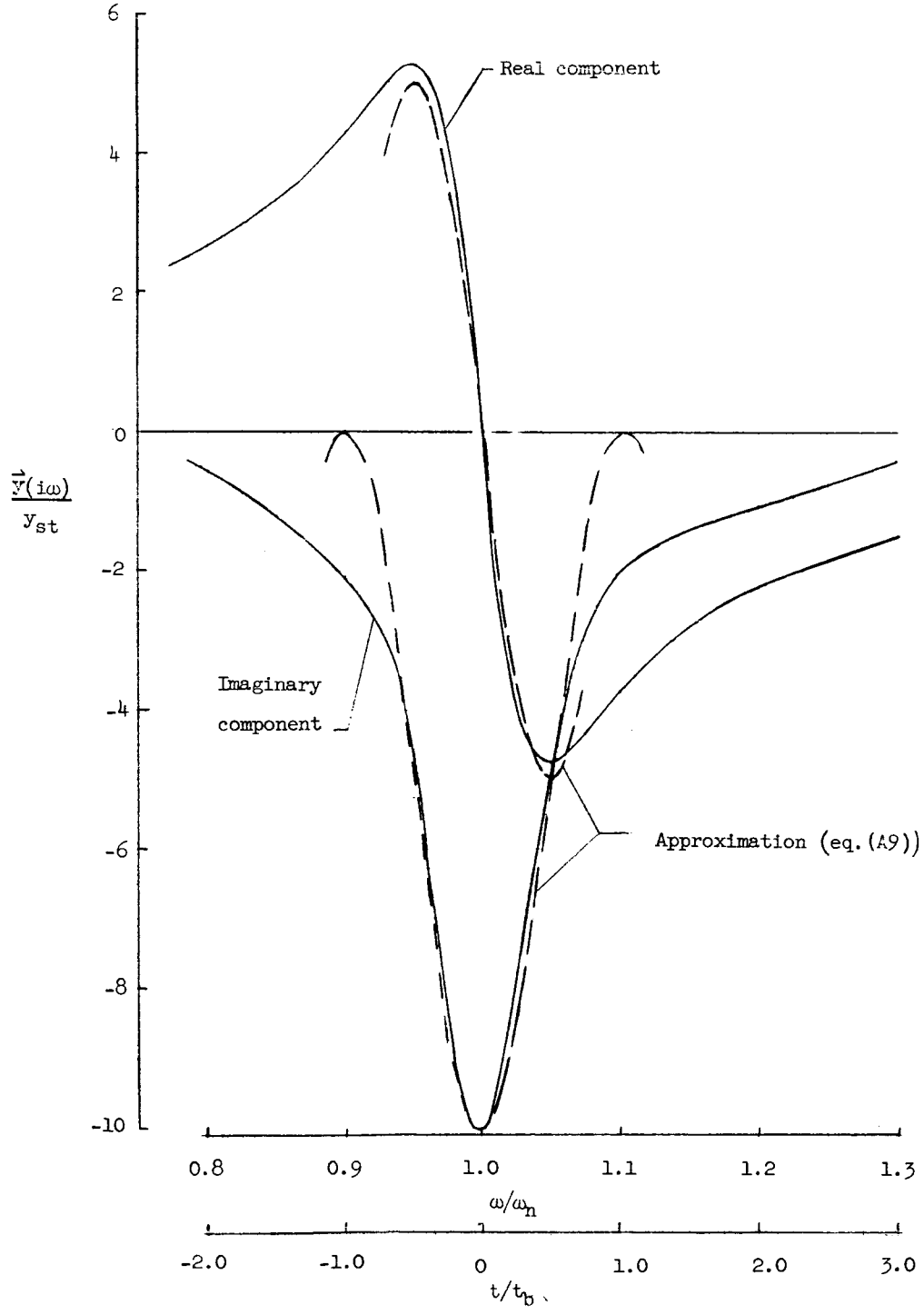

Figure 18.- Vector components of response of a single-degree-of-freedom system. $\zeta = 0.05$.